

1 **Describing posterior distributions of variance components:**

2 **Problems and the use of null distributions to aid interpretation**

3 Joel L. Pick^{1,2,3*}, Claudia Kasper⁴, Hassen Allegue⁵, Niels J. Dingemans⁶, Ned A.
4 Dochtermann⁷, Kate L. Laskowski⁸, Marcos R. Lima⁹, Holger Schielzeth¹⁰, David F.
5 Westneat¹¹, Jonathan Wright¹, Yimen G. Araya-Ajoy^{1,3}

6 ¹ Centre for Biodiversity Dynamics (CBD), Department of Biology, Norwegian University
7 of Science and Technology (NTNU), N-7491 Trondheim, Norway.

8 ² Institute of Ecology and Evolution, University of Edinburgh, Charlotte Auerbach Road,
9 Edinburgh, EH9 3FL, UK

10 ³ Both authors contributed equally

11 ⁴ Animal GenoPhenomics group, Agroscope, Tioleyre 4, CH-1725 Posieux, Switzerland.

12 ⁵ Département des Sciences Biologiques, Université du Québec à Montréal, Montréal,
13 QC, Canada

14 ⁶ Behavioural Ecology, Department of Biology, Ludwig-Maximilians University of Mu-
15 nich, Planegg-Martinsried, Germany

16 ⁷ Department of Biological Sciences, North Dakota State University, Fargo, ND, USA

17 ⁸ Department of Evolution and Ecology, University of California Davis, Davis, CA, USA

18 ⁹ Departamento de Biologia Animal e Vegetal, Centro de Ciências Biológicas, Universi-
19 dade Estadual de Londrina, Londrina, Brazil

20 ¹⁰ Institute of Ecology and Evolution, Friedrich Schiller University Jena, Jena, Germany

21 ¹¹ Department of Biology, University of Kentucky, Lexington, KY, USA

22 ¹² Members of the SQuID working group

23 * Corresponding author, email address: joel.l.pick@gmail.com

24 **Running title:** Null distributions for variance components

25 **Keywords:** hierarchical models, variance, null distribution, permutation, simulations,
26 squidSim

27 **Data and code availability** All code and generated data for the simulated examples
28 are deposited in https://github.com/squidgroup/null_distributions

29 1 Abstract

30 Assessing the biological relevance of variance components estimated using MCMC-based
31 mixed-effects models is not straightforward. Variance estimates are constrained to be
32 greater than zero and their posterior distributions are often asymmetric. Different mea-
33 sures of central tendency for these distributions can therefore be very different, and cred-
34 ible intervals cannot overlap zero, making it difficult to assess the the size and statistical
35 support for among-group variance. This is often done through visual inspection of the
36 whole posterior distribution, and so relies on subjective decisions for interpretation. We
37 use simulations to demonstrate the difficulties of summarising the posterior distributions
38 of variance estimates from MCMC-based models. We compare commonly used summary
39 statistics of posterior distributions of variance components showing that the posterior
40 median is predominantly the least biased. We also describe different methods for gener-
41 ating null distributions (i.e. a distribution of effect sizes that would be obtained if there
42 was no among-group variance) that can be used to aid in the interpretation of variance
43 estimates. We further show how null distributions could be used to derive a p-value that
44 provides complimentary information to the commonly presented measures of central ten-
45 dency and uncertainty and also facilitates the implementation of power analyses within
46 an MCMC framework.

2 Introduction

Estimating variance components using mixed-effects models is common in ecology and evolution (Bolker *et al.*, 2009; Harrison *et al.*, 2018). Mixed-effect models are a flexible statistical tool used to study hierarchically structured data, including extensions for estimating quantitative genetic parameters (animal models; Henderson, 1988; Kruuk, 2004) and comparative analysis (meta-analysis and phylogenetic mixed models; Hadfield & Nakagawa, 2010). Markov chain Monte Carlo (MCMC) algorithms are increasingly used to fit mixed-effects models, due to their flexibility and availability of open-source software (e.g. winBUGS (Gilks *et al.*, 1994), JAGS (Plummer, 2003), MCMCglmm (Hadfield, 2010), Stan (Stan Development Team, 2022b)). MCMC algorithms are a collection of probabilistic simulation methods for generating observations from designated statistical distributions and are typically implemented within a Bayesian framework (Gelman *et al.*, 2013).

MCMC methods have many advantages in ecology and evolution. For instance, we are commonly interested in derived measures such as a standardised measure of variance (e.g. repeatability, heritability and evolvability Nakagawa & Schielzeth, 2010; Houle, 1992). These derived measures can be estimated using the whole posterior distribution of their components, allowing uncertainty to be propagated both within and among analyses. In contrast, in a maximum likelihood framework, the methods to estimate the uncertainty of derived metrics (such as the delta method) can be biased with small sample sizes (O’Hara *et al.*, 2008). Data in ecological and evolutionary studies are also commonly non-Gaussian, for example counts (e.g. number of offspring), binary and ratio data (e.g. survival, presence/absence, sex ratio) and categorical data (e.g. colour morphs, horn type in sheep). The performance of MCMC algorithms in generalized linear mixed-effects models has been found to be superior in terms of accuracy and precision compared with Restricted Maximum Likelihood (REML) approaches (O’Hara & Merilä, 2005; de Villemereuil *et al.*, 2013). Bayesian methods also allow existing information to be incorporated as a prior

74 distribution, although this has rarely been used in ecological or evolutionary studies
75 ([Lemoine, 2019](#)).

76 Despite these clear advantages, there are several issues that empiricists face when
77 using MCMC mixed-effect models. Here we address the issue that variance estimates and
78 their uncertainty can be hard to describe and interpret, especially when trying to assess
79 their biological relevance. We highlight two problems that can occur when estimating
80 variance components, both of which centre around the difficulty of describing the posterior
81 distribution of variance components using summary statistics: (i) finding an appropriate
82 measure of central tendency; and (ii) assessing the statistical support for non-zero among-
83 group variance. These problems stem from variance estimates being constrained to be
84 greater than zero and that their posterior distributions are often asymmetric.

85 In order to describe the posterior distribution, we often present some measure of cen-
86 tral tendency alongside some measure of uncertainty (quantile-based intervals or Highest
87 Posterior Density (HPD) intervals). The posterior mean, median and mode have all been
88 used as measures of central tendency, and more recent works have suggested the general
89 use of the posterior median ([Gelman *et al.*, 2020](#); [McElreath, 2020](#)). There is, however,
90 no clear guidance on which measure provides a more appropriate summary statistic for
91 variance components, although in our experience the mode and mean are most commonly
92 reported. When the posterior distribution of a variance component is far away from zero
93 and is symmetric, then the mean, median and mode are approximately equal (Figure
94 [1a](#)) and inferences are robust to the choice of central tendency metric. However, when
95 variances are small (relative to the total variance) and/or there are small sample sizes
96 (both of which often occur in ecology and evolution), the posterior distributions can be
97 close to zero. As variances are constrained to be greater than zero, these posterior dis-
98 tributions are typically asymmetric and can even be bimodal. Consequently, there can
99 be a considerable difference between the mean, median and mode, with the mode often
100 lying close to zero (Figure [1b](#)). This discrepancy makes it is difficult to draw inference

101 about the magnitude of the posterior variance estimate.

102 Use of the posterior mode is often justified as being the closest to the maximum like-
103 lihood estimate (MLE) when uninformative priors are used. However, this comparison
104 refers to the joint posterior mode, rather than the marginal mode that is typically esti-
105 mated and reported. In more complex models, the joint and marginal modes may differ
106 (Held & Sabanés Bové, 2020, Section 6.5.4), meaning that the marginal mode and MLE
107 are no longer the same. As shown in Figure S2, the convergence of the posterior mode
108 and MLE also requires the use of uninformative improper priors, which are generally not
109 advised (Gelman *et al.*, 2013) and are thus seldom used. The posterior mode is also hard
110 to estimate; it is typically done using kernel density estimation and different methods
111 may provide quite different estimates (Figure 2), thereby providing an additional source
112 of hidden ambiguity. Furthermore, the mode requires a larger number of samples in
113 the posterior distribution to be reliably estimated, and will show greater variation be-
114 tween models/chains run on the same dataset (Kruschke, 2015). In contrast, the mean is
115 strongly affected by extreme values, and so by the long tail of an asymmetric distribution.

116 It is also often important to assess statistical support for among-group variance at a
117 particular level. Typically 95% credible intervals (CRIs) are presented as a measure of
118 uncertainty in parameter estimates derived from MCMC model fits. As variance com-
119 ponents cannot overlap zero, CRIs give no information about the compatibility of the
120 estimates with the null hypothesis (no among-group variance). Posterior distributions
121 are often inspected visually, as histograms or density plots, in order to assess whether the
122 distributions are biased towards zero, which is commonly assumed to signify that the es-
123 timated variance is not different from zero. What is seldom appreciated, however, is that
124 the degree of smoothing that is applied in such plots (via the binning interval or band-
125 width) can alter these conclusions. This means that the same distribution can be seen
126 as uni- or bimodal, or peaking at zero or away from zero (Figure 2). Such assessments
127 therefore tend to be highly subjective and lack a proper quantitative basis.

128 To address this, several methods for generating metrics for assessing the confidence
129 in a result (such as p-values) have been suggested in a Bayesian framework (reviewed
130 in [Makowski *et al.*, 2019a](#)). Two of these, Region of Practical Equivalence (ROPE) and
131 Bayes factors, can be used for variance components. The ROPE approach identifies a
132 range of values considered negligible or too small to be of any practical relevance (i.e. the
133 Region of Practical Equivalence), and quantifies the proportion of overlap between the
134 posterior distribution and the ROPE. This is similar to equivalence testing in a Frequen-
135 tist framework, specifically to the two one-sided tests (TOST) approach ([Lakens *et al.*,
136 2018](#)). Bayes factors are analogous to Frequentist likelihood ratios, comparing different
137 models (for example with and without the random effects of interest), but unlike likeli-
138 hood ratios they incorporate information from the prior distributions into the comparison
139 of the models ([Morey *et al.*, 2016](#)). Both of these metrics can be used to provide a mea-
140 sure of statistical support for estimates of variance components, but their implementation
141 is complicated - ROPE requires the definition of a threshold, incorporating further sub-
142 jectivity into the analysis, whilst the computation of Bayes factors can be challenging,
143 and even not implementable in some commonly used programs (e.g. MCMCglmm). We
144 discuss these two methods further in the discussion.

145 Here we suggest a complementary method to assess statistical support in mixed-effect
146 models, which compares the estimated variance components to a null distribution in
147 order to inform the statistical inferences made from the model. This involves creating a
148 distribution of effect sizes that would be expected under the null hypothesis (no among-
149 group variance) and comparing this null distribution with the observed among-group
150 variance. This method has several advantages. Null distributions can be used to generate
151 a p-value describing the probability that the observed estimate is as or more extreme than
152 expected under the null hypothesis. Although often criticised through their association
153 with Null Hypothesis Significance Testing (NHST; [Wasserstein & Lazar, 2016](#); [Amrhein
154 *et al.*, 2017](#); [McShane *et al.*, 2019](#); [Amrhein *et al.*, 2019](#)), p-values have well understood
155 and useful properties. When correctly interpreted, these test statistics provide a useful

156 tool by indicating how consistent an observed effect size is with a scenario in which there
157 is no among-group variance. In contrast to the ROPE method, the creation of a null
158 distribution requires no subjective decisions about thresholds and, in contrast to Bayes
159 Factors, they can be implemented using the output from any Bayesian model.

160 We present two methods, permutation and simulation, for generating null distributions
161 for variance components. When generating a null distribution using permutation, some
162 feature of the data or data structure is randomised to produce a new dataset that contains
163 the structure of the original dataset, but where there is no relationship between the
164 response variable and the variable of interest (the among-group variance in this case).
165 This randomization is repeated a large number of times (e.g. 1000) to create many
166 different permuted datasets. The same analysis is then carried out on the permuted
167 datasets as on the original dataset, and a test statistic of interest (e.g. the estimate of
168 among-group variance) is used to create a null distribution of test statistics (Figure 1c,d).
169 A (one-tailed) p-value can then be derived as the proportion of permuted datasets with
170 a test statistic greater than or equal to the test statistic observed with the real data set.
171 Permutation tests have already been suggested as an alternative to likelihood ratio tests
172 for frequentist analyses (Fitzmaurice *et al.*, 2007; Samuh *et al.*, 2012), although they are
173 not commonly utilized in ecology and evolution (but see Araya-Ajoy & Dingemanse, 2017;
174 Stoffel *et al.*, 2017). Permutation tests are a subclass of nonparametric tests (Pesarin
175 & Salmaso, 2010; Lehmann & Romano, 2005) and do not rely on specific probability
176 distributions, and so make few assumptions. However, as we show later in the manuscript,
177 datasets can be permuted in several different ways when the data structure is complex,
178 and the consequences of the choices involved in such cases are often not immediately
179 obvious. An alternative method of creating a null distribution is using simulations. This
180 process is similar to permutation, but instead of generating permuted datasets we can
181 simulate datasets from the observed model parameters (in a similar way to parametric
182 bootstrapping), whilst setting the variance in question to zero. This simulation method
183 makes more assumptions about the data and model, but allows for more control of the

184 manipulated features of the simulated datasets compared with permutations.

185 Finally, a crucial part of designing experiments and statistical analyses is assessing
186 the power to detect an effect size of interest. Power is defined as the probability of
187 rejecting the null hypothesis (i.e. no among-group variance) for a given effect size at
188 a specified alpha level (typically 0.05), and so is dependent upon the generation of p-
189 values. Although power relates to NHST and the often criticized alpha level ([Wasserstein](#)
190 [& Lazar, 2016](#); [Amrhein *et al.*, 2017](#); [McShane *et al.*, 2019](#); [Amrhein *et al.*, 2019](#)), it
191 and analogous metrics ([Gelman & Carlin, 2014](#)) remain an important tool for study
192 design regardless of statistical philosophy, and this is because it provides a quantitative
193 approach to calculating optimal sample sizes and designing sampling regimes. Power may
194 also provide a more useful metric than precision when considering variance components.
195 As their distributions are bounded at zero, standard errors will always decrease when
196 distributions are close to zero (see Supplementary Figure S4). However, the concept
197 of power for variance components in MCMC models is not well developed. As null
198 distributions can be used to generate p-values, they also provide a convenient way of
199 conducting power analysis.

200 Here, we first compare commonly used summary statistics of posterior distributions
201 of variance components. We then demonstrate the utility of null distributions (i.e. a
202 distribution of effect sizes that would be obtained if there was no among-group variance)
203 to generate a complementary p-value statistic and aid the interpretation of the variance
204 components. Comparison with a null distribution provides a quantitative measure of
205 confidence that the observed variance component is larger than what might be expected
206 under the null hypothesis, given the data structure and priors used. Importantly, we
207 are not advocating that this approach should replace the presentation and use of ef-
208 fect sizes (e.g. posterior mean/median/mode) and credible intervals, but rather that it
209 should be used as an additional and complementary statistic. Finally, we show how null
210 distributions can be used to perform a power analysis within an MCMC framework.

211 **3 Methods**

212 **3.1 Generation of Simulated Datasets**

213 Simulated datasets were generated out in R (version 4.1.0 [R Core Team, 2022](#)) using
214 the squidSim R package (version 0.1.0 [Pick, 2022](#)). We first simulated Gaussian data
215 with one hierarchical level and varied the number of observations per group (2 and 4)
216 and the number of groups (20, 40 and 80). We simulated a total variance of 1 and
217 varied the among-group variance (0, 0.1, 0.2 and 0.4; since the total variance simulated
218 was 1, these are also the respective intra-class correlations (ICCs)/repeatabilities). We
219 simulated every combination of these parameters (24 parameters sets) and for each set we
220 simulated 500 datasets. Power to detect among-group variance is known to be determined
221 by effect size and sample size both within and among groups. We deliberately chose these
222 parameter values and sample sizes to explore scenarios where power is low ([Dingemans &
223 Dochtermann, 2013](#)) to understand the impact on posterior distributions. These sample
224 sizes also correspond to typical experimental designs in behavioral ecology or life history
225 data collected on wild populations ([Bell *et al.*, 2009](#)).

226 We analysed each simulated dataset with a linear mixed-effect model specifying group
227 level random effects in a Bayesian framework, using Stan with the rstan package (version
228 2.21.3 [Stan Development Team, 2022a](#)). We specified weakly informative priors on the
229 among-group and residual standard deviations (half-Cauchy distribution with scale 2),
230 and ran one chain for each model with 5000 iterations and a warm-up period of 2000
231 iterations. Across the majority of models (95%) this ensured an effective sample size
232 in the posterior distribution of the among group variance of >500 . For comparison, we
233 also ran REML models using the lmer function of the lme4 package (version 1.1-29 [Bates
234 *et al.*, 2015](#)), the results of which are shown in the Supplementary Figure [S1](#).

235 As a demonstration that our findings hold with more complex data, we simulated
236 Bernoulli data (binomial with one observation) with 80 groups and 4 observations per

237 group. Among-group effects were simulated from a Gaussian distribution on the latent
238 scale, with among-group variances of 0 and 0.2. The latent scale response variable was
239 then transformed using the inverse logit function to provide the probabilities, and sampled
240 with a Bernoulli process. We simulated 100 datasets for each variance, and analysed the
241 data as outlined above.

242 **3.2 Comparison of Posterior Distribution Summary Statistics**

243 From the posterior distributions of the among-group variances, we calculated the posterior
244 mean, median and mode, and compared these estimates with the simulated values.

245 While calculating the mean and median of the posterior distribution is straightfor-
246 ward, there are several ways of estimating the mode of the marginal posterior distribution,
247 which involve some (hidden) assumptions. Commonly used functions in R include the
248 `posterior.mode` function in the MCMCglmm package (Hadfield, 2010), the `Mode` func-
249 tion in the ggdist package (Kay, 2022), and the `map_estimate` function of the bayestestR
250 package (Makowski *et al.*, 2019b). Typically these functions estimate the mode by es-
251 timating the parameter value at which the kernel density is maximised. Kernel density
252 estimation essentially involves fitting a model to the distribution of posterior samples
253 to estimate a density function. The maximum of this function (the estimated mode) is
254 then calculated over a series of predicted values. One key parameter in kernel density
255 estimation is the bandwidth, which essentially describes the amount of smoothing and
256 is analogous to the number of breakpoints in a histogram (Figure 2). Common meth-
257 ods generally scale bandwidth generated by specific algorithms. MCMCglmm scales the
258 bandwidth generated by Silverman’s ‘rule of thumb’ algorithm (nrd0; eqn 3.31 in Sil-
259 verman, 1986) by 0.1 (i.e. it is much less smoothed; Figure 2d). In contrast, ggdist
260 and bayestestR use the default values of the nrd0 and SJ algorithms (Sheather & Jones,
261 1991), respectively (the default bandwidth of the nrd0 algorithm is also used by `density`
262 function in R; Figure 2a). The impact on the potential inferences caused by the choice

263 of scaling is demonstrated in Figure 2, with the degree of smoothing affecting where the
264 posterior mode is estimated. To explore this impact of bandwidth, we estimated the
265 posterior mode using these two bandwidth scalings (0.1 and 1). The kernel density was
266 estimated using the SJ algorithm (Sheather & Jones, 1991), and the mode was estimated
267 using 512 predicted values with a cut point at zero. These additional parameters all differ
268 between commonly used functions, but have much smaller impacts upon the results than
269 the bandwidth, and so we hold them constant here.

270 To ensure that our results, especially on the mode, were not driven by the choice of
271 the prior, we ran additional models on a subset of the data (ICC=0.2, N groups=80,
272 N within=2) with a half-Cauchy prior with scale 5 and 25, and uniform priors from 0
273 to 5 and 0 to 25 on the among-group standard deviation. The half Cauchy prior has
274 been recommend for variance components (Gelman, 2006) and is commonly used (note
275 it is equivalent to the parameter expanded priors in MCMCglmm). For demonstration
276 purposes, we also ran models in MCMCglmm specifying uninformative improper priors.
277 Given the simplicity of these models, the posterior mode is expected to correspond to the
278 REML estimate. The different parametrizations of the half Cauchy and uniform priors
279 resulted in no difference in the results (Figure S2). As expected, using an uninformative
280 improper prior led to a concordance between REML and posterior mode, although the
281 strength of this similarity differed between the different methods used to estimate the
282 mode (Figure S2).

283 To compare these different measures of central tendency, we calculated the bias as
284 $\frac{1}{n} \sum \hat{\theta}_i - \theta$ (where θ is the true simulated value, $\hat{\theta}_i$ is the model estimate from i th simulation
285 in a parameter set, and n is the number of simulations). For the non-zero effect sizes,
286 we also calculated relative bias $\frac{1}{n} \sum \frac{\hat{\theta}_i - \theta}{\theta}$ and absolute relative bias $\frac{1}{n} \sum \frac{|\hat{\theta}_i - \theta|}{\theta}$. We also
287 calculated the precision as $1/\sqrt{\frac{1}{n} \sum (\hat{\theta}_i - \bar{\theta})^2}$, which we present in the Supplementary
288 Figure S4.

289 3.3 Creation of null distributions and p-values

290 We created null distributions for each simulated dataset using two methods. First, we
291 permuted the datasets by shuffling the group indices (IDs) to create 100 new datasets,
292 each of which was analysed in the same way as the original dataset. From each permuted
293 dataset, we extracted the same parameters (the estimates of central tendency in the
294 posterior distribution of the among-group variance) as for models fitted to the original
295 data and created the corresponding null distributions. Second, we used simulations to
296 create the null distribution. To do this, we simulated datasets with no among-group
297 variance. To ensure the same total variance we added the posteriors of the among-group
298 and residual variances of the original model, and we used the median of the resulting
299 distribution as our inputted value for the simulated residual variance in the null model.
300 The choice of the median for this step should have little consequence, as this derived
301 distribution will be estimated with much less uncertainty and so will be symmetric,
302 meaning that the three measures of central tendency will be equivalent. Each simulated
303 null dataset was analysed in the same way as the original dataset, and we extracted the
304 same parameters to create the corresponding null distributions.

305 Although we recommend using a larger number of permutations/simulations to build
306 up a null distribution in empirical studies (e.g. 1000), here we used 100 permutations and
307 simulations to generate null distributions for these simulated datasets in order to reduce
308 the computational burden (500 simulations for 4 variances, with 6 different sample sizes is
309 12000 datasets, for each of which we performed 100 permutations and 100 simulations).
310 We then calculated a p-value for each original dataset, as the proportion of estimates
311 in the null distribution that were higher than the estimate from the original data. We
312 calculated p-values using each central tendency measure, and these are compared in
313 Figure S5.

314 3.4 Power analysis

315 Using the simulated datasets outlined above, we compared two ways by which power can
316 be calculated. Power is defined as the probability of rejecting the null hypothesis (i.e. no
317 among-group variance in this case) for a given effect size and data structure at a specified
318 alpha level (typically 0.05). To do this, we calculated the proportion of datasets in which
319 the p-value was below a nominal threshold of 0.05. It is worth noting that, although
320 power has a superficial connection with NHST, power can also be seen as a description
321 of the distribution of p-values expected for a given effect size and data structure. Other
322 descriptions of this distribution (e.g. the mean) would be simple functions of the power.
323 We therefore chose to present power as a description of the distribution of p-values as it
324 is conceptually well understood and frequently used, rather than due to any philosophical
325 alignment with NHST.

326 First, we estimated power using the p-values generated through comparison with the
327 null distributions from both permutation and simulation approaches outlined above ('full'
328 method). We were also able to calculate the false positive rate for this method (essentially
329 the power when the simulated value is 0). Second, we used the model estimates from the
330 simulated datasets with zero among-group variance for each data structure (combination
331 of among- and within-group sample sizes) as a null distribution, against which the es-
332 timates from simulated datasets with among-group variance could be tested ('reduced'
333 method). This method of estimating power is similar to the simulation method of gen-
334 erating null distributions, but involves generating one null distribution for *all* datasets
335 with the same data structure, instead of null distribution for *each* dataset. It is therefore
336 massively less computationally intensive for power analyses, because to explore power
337 within the parameter space presented here it only required the running 12,000 models,
338 rather than 1,212,000. It is not possible to calculate a false positive rate for this method,
339 as this would involve comparing the null distribution with itself, and so the false positive
340 rate would be 5%, by definition.

341 4 Results

342 4.1 Comparing summary statistics of the posterior distribution

343 When the simulated among-group variance was zero, all summary statistics were up-
344 wardly biased to some extent (the posterior distribution cannot include 0; Figure 3a).
345 Predictably, the posterior mean and median from datasets with zero variance were con-
346 siderably more upwardly biased for small sample sizes, in contrast to the mode. The
347 mean was the most biased as it is heavily influenced by the tail of the distribution. Con-
348 sequently, this upward bias is stronger when the uncertainty is high (i.e. when the tail is
349 large). Note, however, that this upward bias is also present in Frequentist analyses (see
350 Figure S1), and is not just a feature of Bayesian analyses.

351 When the simulated among-group variance is non-zero, then the mean, median and
352 mode all appeared to be consistent estimators, in that any bias occurred only at small
353 sample and/or effect sizes. The posterior median generally converged on the simulated
354 value at lower effect and sample sizes (Figure 3b), as compared with the posterior mean,
355 which was upwardly biased, and the posterior mode that was biased towards zero (Figure
356 3b).

357 When considering the absolute relative bias (Figure 3c), the mean and median show
358 very similar levels of bias, with exception of the lowest sample and effect size combination
359 where the mean was more biased. This suggests that although the mean is more likely to
360 be upwardly biased, the magnitude of the bias is similar in the two measures. However,
361 the mode is consistently more biased than the other measures (Figure 3c), although
362 this bias disappears at higher sample and effect sizes. Following the example shown in
363 Figure 2, the bias in the mode depends upon the bandwidth that was used, with higher
364 smoothing showing less bias across the two bandwidths tested. We found similar patterns
365 in our Bernoulli simulations (Figure 5a).

366 4.2 Performance of the null distributions

367 As expected, both permutation and simulation methods produced a uniform distribution
368 of p-values when applied to datasets where the simulated among-group variance was zero
369 (Figures 4). The distribution of p-values from both tests then shifts towards zero as the
370 sample size and the magnitude of the variance increase (Figure 4). Similar patterns were
371 found in the Bernoulli simulations (Figure 5b).

372 Importantly, although the mean, median and mode were often quite different in magni-
373 tude (reflecting skew in the posterior distribution), the inference based upon the p-values
374 did not differ between the different metrics. There were strong correlations between p-
375 values estimated with the different metrics, with the exception of the mode estimated
376 with less smoothing (see Figures S5 and S7). P-values were also strongly correlated
377 between null distributions generated through simulation and permutation methods (see
378 Figures S6 and S8).

379 4.3 Power analyses

380 When considering the full method of estimating power, both ways of generating null
381 distributions (permutation and simulation) gave very similar results (Figure 6), with
382 marginally higher power for the permutation method. These power estimates are very
383 similar to previous published estimates for Frequentist models (Dingemans & Dochter-
384 mann, 2013). These methods also displayed the expected false positive rates (5%) under
385 all simulated conditions (black points in Figure 6). The reduced method for estimating
386 power, using the same null distribution for all simulation datasets within a particular
387 data structure, generally gave a similar power to the other methods (Figure S9).

388 As with the p-values, power was not particularly sensitive to the measure of central
389 tendency used, the highest power being seen in the mode with higher smoothing and the
390 lowest power with the mode with less smoothing (Figure S9).

391 5 Worked example - Random slopes

392 As is often the case, the examples presented above are simplistic and empiricists com-
393 monly encounter more complex questions and data structures in their studies. Here we
394 outline a more realistically complex example where the permutation of datasets require
395 some careful decisions.

396 Random slope models (where group-specific intercepts and slopes are modelled, also
397 known as random regression) provide a good example of this complexity. We will fo-
398 cus here on generating a null distribution for the estimate of among-group variance in
399 slopes. This estimate is based upon the relationship between the predictor variable and
400 response, the distribution of the response variable across groups, and the distribution of
401 the predictor variable within and across groups. This provides us with four possibilities
402 for permutation: 1) permuting the response variable (retains data structure and breaks
403 all relationships with response); 2) permuting the predictor (retains the group data struc-
404 ture, breaks link between predictor and response, and the distribution of the predictor
405 across groups); 3) permuting the group identities (breaks the group data structure, but re-
406 tains link between predictor and response); and 4) permuting the predictor within groups
407 (retains the group data structure and the distribution of the predictor across groups, but
408 breaks link between predictor and response). Additionally, we can also generate a null
409 distribution through simulation, where we can simply simulate no among-group variance
410 in slopes, adding the variance generated by the random slopes to the residual to ensure
411 the same total phenotypic variance. Below we explore these different null distributions
412 using a simulated and a real data set. Null distributions were generated based upon the
413 analyzes of 100 null datasets.

414 5.1 Simulated dataset

415 We imagined a hypothetical researcher measuring the body mass of a bird species at
416 different times of the day with the aim of studying how temperature affects body mass.
417 The question of interest was to assess whether there is variation among individuals in
418 how temperature affects their body mass. The (simulated) observed data set consisted of
419 300 individuals measured 4 times each. Body mass and temperature were both normally
420 distributed. Temperature was scaled to have a mean of 0 and variance of 1, and has an
421 effect on body mass of 0.2 for the average individual. The simulated among individual
422 variance in the intercepts was 0.2 and the phenotypic variance generated by variation
423 in slopes was 0.1 (with no correlation among random slopes and intercepts), while the
424 residual variance was set to 0.7 to ensure a total phenotypic variance not explained by
425 the average effect of the environment was 1. Formulas to estimate the total phenotypic
426 variance in random slope models can be found in [Allegue *et al.* \(2017\)](#) There were no
427 systematic differences in the average temperature experienced by the different individuals.

428 5.2 Real world dataset

429 For our example with real data, we used a study on variation in the plastic aggressive
430 response to intruders of great tits (*Parus major*) in a nestbox population in southern
431 Germany ([Araya-Ajoy & Dingemanse, 2017](#)). Aggressiveness data were collected over a
432 6-year period (2010–2015) for all male birds during their first breeding attempt each year.
433 The aggression test started when a taxidermic mount of a male great tit was presented on
434 a 1.2 m wooden pole with a playback song 1 m away from the subject's nest box. They
435 subsequently recorded the behaviour of the focal male for a period of 3 min after it had
436 entered a 15 m radius around the box. Simulated territorial intrusions were performed
437 twice during the egg-laying stage and twice during the egg-incubation stage of each focal
438 nest. Therefore, males had repeated measures both within- and among-years.

439 We analysed 2854 aggression tests performed to 1042 breeding attempts of 679 in-
440 dividuals. The average number of years for which we obtained an individual’s reaction
441 norm was 1.4, with 513, 142, 44, 8, 8 and 1 individual(s) sampled for one, two, three, four,
442 five or six breeding attempt(s) (years), respectively. On average, we acquired 2.8 (out of
443 4) data points for male aggressiveness per breeding attempt (i.e. year), because males
444 did not always respond to the territorial intrusion experiment (Araya-Ajoy & Dingem-
445 manse, 2017). Details of the experimental setup, and assayed behaviours, are provided in
446 Araya-Ajoy & Dingemans (2014). For the purpose of this paper, we used the subject’s
447 minimum distance to the mount as a measure of aggressiveness because previous work
448 implies that this behaviour represents a reliable predictor of the intensity of an aggressive
449 response in both stages of breeding (Araya-Ajoy & Dingemans, 2014).

450 5.3 Random slope methods

451 Both datasets were analysed using random slope mixed-effects models, specifying the en-
452 vironmental predictor (temperature for the simulated example and breeding stage for the
453 real example) as a fixed covariate, and random intercepts and environment slopes across
454 individuals. We then generated 5 null distributions (4 permutations and 1 simulation),
455 as outlined above, with which we compared the estimate of among individual variance in
456 slopes from the observed data. Breeding stage (egg-laying versus egg-incubation) was first
457 coded as zero (for laying) versus one (for incubation), and subsequently mean centred and
458 standardized to standard deviation units. Models were fitted in a Bayesian framework,
459 using Stan with the rstan package (version 2.21.3 Stan Development Team, 2022a). We
460 specified weakly informative priors on the among-group and residual standard deviation.
461 We ran three chains for the model of the simulated and real observed data with 5,500
462 iterations and a warm-up period of 500 iterations. To decrease computational burden,
463 the models for the permuted/simulated data sets were run for only one chain. We then
464 generated five null distributions of posterior medians for each dataset, using the methods

465 described above.

466 **5.4 Random slope results**

467 The different types of null distributions provided the same qualitative results, support-
468 ing the conclusion regarding among-individual variation in slopes, in both the real and
469 simulated datasets (Fig 7). For these datasets, permuting individual identity created
470 null distributions with a larger mean value of random slope variance (see Discussion for
471 an explanation). It is important to note that these results relate only to this specific
472 example and may not generalize to other studies. We therefore recommend exploring the
473 particular consequences of using different types of permutations for specific datasets, if a
474 reader wishes to use a permutation method.

475 **6 Discussion**

476 Through the use of simulations, we demonstrate the difficulties of summarising the poste-
477 rior distributions of variance estimates from MCMC-based models. We describe different
478 methods for generating null distributions that provide useful complimentary informa-
479 tion alongside the presentation of central tendency and uncertainty that are generally
480 reported. We also show a way in which null distributions could be used to derive a p-
481 value, which is an easy addition to the statistics presented when summarizing a posterior
482 distribution and also facilitates power analysis.

483 **6.1 Summary statistics**

484 Our experience in ecology and evolution is that both posterior mean and mode are com-
485 monly, but inconsistently, presented without justification. For fixed effect parameter
486 estimates, this is typically inconsequential, as the posteriors are usually symmetrically

487 distributed. When estimating variance components, however, our simulations show that
488 depending upon the underlying parameter value, both of these measures can show large
489 biases in opposite directions. When posterior distributions are close to zero and there
490 *is* among-group variance, the posterior mode is very biased towards zero, whereas the
491 posterior median and mean perform much better. On the other hand, if there is no
492 among-group variance, the mode is by far the least biased. The mode, however, suffers
493 further from subjectivity in its estimation. Our simulations also show that the estimation
494 of the mode depends on the underlying algorithm for mode estimation. Unfortunately,
495 the method of mode estimation is rarely justified or even stated in empirical papers. The
496 mode also requires larger posterior distributions to be reliably estimated and will show
497 greater variation between models/chains (Kruschke, 2015). Given this hidden ambiguity
498 in the estimation of the mode, we would therefore cautiously recommend the presentation
499 of the posterior median, or both median and mean, as a measure of central tenancy for
500 variance components. This recommendation is based upon the median being generally
501 less biased than the mean when power is low. Presenting both allows the discrepancy to
502 be seen, showing that the distribution is near to zero and not symmetric, further stressing
503 the uncertainty in these measures.

504 Upward biases in variance components have been seen before when power is low, but
505 the dependence on the choice of the central tendency metric has not been highlighted.
506 For example, Fay *et al.* (2022) note overestimation of variance components in Bernoulli
507 models, with this overestimation decreasing in size as sample size and effect size increase.
508 Fay *et al.* (2022) use the posterior mean as a summary statistic, and (as we show in
509 Supplementary Figure S10) this bias will decrease (although not disappear completely)
510 through the use of a posterior median. This is not just a bias in Bernoulli models, or in
511 fact MCMC models (Figure S1), but a general property of variance components estimated
512 with low power.

513 It is often argued that rather than presenting summary statistics, we should present

514 and interpret the whole posterior distribution, which are frequently presented using den-
515 sity plots. Again, the underlying parameters of the kernel density estimation are usually
516 not presented alongside the density plots, meaning the amount of smoothing is not doc-
517 umented. A large degree of smoothing can hide asymmetry and/or bi-modality, and so
518 change inferences. We therefore suggest the use of histograms over density plots in the
519 presentation of posterior distributions, because although they are subject to the same
520 smoothing problems, the degree of smoothing is explicit in the histogram, but hidden in
521 the density plot. Alternatively, other plots that explicitly show the raw posterior samples
522 (e.g. beeswarm plots) could be used (e.g. Figures 4 and 5).

523 6.2 Null distributions

524 The null distribution approaches outlined here are relatively easy to use, and allow quan-
525 tification of confidence that a variance estimate is the result of a biological process rather
526 than a consequence of the choice of priors and data structure. Importantly, the p-values
527 based upon null distributions are not dependent upon what measure of central tendency
528 is used. Such inferential statistics comparing the observed estimates with the null distri-
529 butions can provide quantitative measures that can be reported alongside the observed
530 estimates and uncertainty, and provides a useful tool for assessing the probability that
531 variance components are non-zero and thereby supplement visual inspections of posterior
532 distributions, or comparison of posterior mode, median and mean. Furthermore, they
533 can serve as an objective and easy-to-communicate assessment of the biological relevance
534 of an estimated variance component to the general public and policy makers, or for the
535 statistical support of non-zero values for derived statistics like heritability, repeatability
536 or evolvability. Common criticisms of p-values include that they are often misinterpreted
537 or used for NHST. We would therefore recommend readers thinking of using the null
538 distribution approach to acquaint themselves with the literature on these topics (some
539 useful examples include [Wasserstein & Lazar, 2016](#); [Amrhein *et al.*, 2017](#); [McShane *et al.*,](#)

540 [2019; Amrhein *et al.*, 2019](#)). Importantly, p-values cannot demonstrate absence of effect,
541 just confidence in difference from the null hypothesis (here no among-group variance).
542 We believe generating null distributions will help empiricists understand these concepts,
543 as they can be used to give a visual representation of what a p-value signifies.

544 As we illustrate in our examples of random slopes, there are different ways of per-
545 muting datasets, which become more varied as the complexity of the data structure and
546 model increase. Our example on random slope analysis demonstrated that these differ-
547 ences can lead to qualitatively similar results, although whether they always or usually
548 do so would require a much broader set of simulations than we report here. Interestingly,
549 permuting individual identity created null distributions with noticeably larger values of
550 random slope variance. We believe this is due to the existence of random slopes in the
551 simulated and real data set generating heterogeneous residuals (i.e. variance in response
552 changed with the environmental predictor) that were confounded with random slope vari-
553 ation in the analyses of the null data sets (similar effects are also shown in [Ramakers
554 *et al.*, 2020](#)). The other permutation methods break up the relationship between the
555 predictor and response, and so the average estimate for the null distributions was lower.
556 This illustrates how comparing the results of the different methods of null distributions
557 generation may provide insights that may be used to inform the statistical inferences
558 from estimated variance components.

559 In some instances, generating a null distribution using permutations may not be
560 possible. For example, in event-history models of survival (where individuals have an
561 entry for each time point where they are observed, in a sequence of 0's for time points
562 they survive and a 1 for the time point after which they die). In this case, permuting the
563 individual identifiers would fundamentally alter the data structure, meaning that some
564 individuals had multiple deaths. This could be made to work in the context of an animal
565 model, where the observed 0's and 1's could be interchanged between individuals, so that
566 the same between individual structure was maintained, but the link with the pedigree

567 was broken. This serves to demonstrate that some care needs to be taken when assessing
568 the suitability of permutations and how they impact the data structure on a case-by-
569 case basis. Overall, we are not advocating a specific recipe for permutations here - it is
570 likely context and question dependent. We instead advocate a simulation approach at
571 the planning stage, using simulations to check in advance that the permutation design
572 gives desired properties with your likely data structure.

573 Generating null distributions through simulation avoids many of the issues with the
574 permutation approach, although it does not account so well for the particularities of each
575 data set. Simulation has the advantage that it allows the structure of the data to be
576 fully retained, a more fine-scale alternation of the variances in question, and it makes
577 no additional assumptions than those already being made by the statistical model itself.
578 Reassuringly, in our random slope example, the null distributions generated using the
579 simulation method were similar to the other methods. We therefore cautiously recom-
580 mend the use of this simulation method, as it is the most flexible for complex models.

581 These null distribution approaches are, however, computationally intensive and ap-
582 plying them can take a long time depending upon the model complexity, the amount
583 of data and the available computational resources. MCMC methods are often used for
584 highly complex problems (e.g. double hierarchical GLMs; [Cleasby et al., 2015](#)), where
585 running a large number of permutations may not be an option. The number of permuta-
586 tions/simulations that are run affects the precision with which a p-value can be calculated
587 and the minimum p-value that can be calculated - a null distribution of 100 can have a
588 minimum p-value of 0.01 and vary by intervals of 0.01. This is why we would recommend
589 a higher number of samples in the null distributions than we used here. However, we
590 were able to produce meaningful results with 100 simulations, and even a few permuta-
591 tions/simulations would give some idea (although much less reliably) of the compatibility
592 of the observed variance with the range expected under the null hypothesis.

593 6.3 Alternative approaches

594 A p-value is defined as the probability that an estimate equal to or more extreme than
595 the observed estimate would occur under the null hypothesis (i.e. if the true among-
596 group variance is zero). It relies upon the distribution of p-values being uniform when
597 the null hypothesis is true, a property that is expected to be invariant to sample size (as
598 we show in Figure 4). P-values therefore provide support for the alternative hypothesis,
599 but they do not provide support for the null hypothesis. The ROPE value and Bayes
600 factors aim to assess actual support for the null hypothesis, and therefore depend upon
601 sample size. Below we outline the potential issues that empiricists may encounter when
602 trying to employ these methods.

603 The ROPE introduces another source of subjectivity into the analysis, because it
604 involves an arbitrary threshold that needs to be defined. This is not trivial in the case
605 of variance components, as small variances can have large knock-on effects. For example,
606 [McFarlane *et al.* \(2015\)](#) find that maternal genetic effects account for 2% of variation
607 in fitness, but this small amount predicts a 56% increase in mean lifetime reproductive
608 success in less than 10 generations, which is highly biologically meaningful. [Bonnet *et al.*](#)
609 [\(2022\)](#) address this by using simulations to demonstrate the biological relevance of the
610 thresholds they use (0.01 and 0.001, for the variances not ICC). There is also discussion
611 about whether the overlap of the whole posterior or the 95% credible interval should
612 be used with ROPE ([Makowski *et al.*, 2019a](#); [Schwaferts & Augustin, 2020](#)). As with
613 NHST, 95% is also an arbitrary cutoff, and so the ROPE would represent the overlap
614 of two arbitrary thresholds. ROPE is often discussed in a context where a cost-benefit
615 analysis can be used to work out the minimum effect size that warrants the use of a
616 particular intervention, for example of medical interventions ([Kruschke, 2018](#)). Typically
617 this is not relevant for research in ecology and evolution as, in many cases, it is of interest
618 whether variance in a particular component exists, and if so its magnitude. We think
619 there is clear application for using ROPE in fields like conservation, where interaction

620 with stakeholders requires thresholds over which decisions need to be made, but for many
621 empiricists, ROPE requires more subjective decisions to be made and justified.

622 Bayes factors can be used to test the 'significance' of parameters in Bayesian mixed-
623 effect models. However, the calculation of Bayes factors that allow inferences to be made
624 about variance components is not straightforward. They require large posterior distri-
625 butions for stable estimation and are sensitive to both prior and model specification
626 (Gelman *et al.*, 2013; Navarro, 2019; Schad *et al.*, 2022). Bayes factors are also not im-
627 plementable in all programs, including commonly used programs in ecology and evolution
628 (e.g. MCMCglmm). Our approach provides an alternative to this method, which is easily
629 implemented and allows straightforward interpretation with reference to the probability
630 that the estimate obtained is the consistent purely with the data structure and model
631 specification.

632 **6.4 Power analysis and possible alternatives**

633 Power analysis is controversial as it relies on NHST. NHST is controversial because its
634 misuse has been attributed to scientific misconduct and the replication crisis (Wasserstein
635 & Lazar, 2016; Amrhein *et al.*, 2017; McShane *et al.*, 2019; Amrhein *et al.*, 2019), issues
636 which relate to the use of p-values *after* data collection and analysis. Power analysis, how-
637 ever, serves a clear purpose in aiding experimental design, and is conducted *pre-analysis*,
638 and so is perhaps not subject to the same criticisms. Suggested alternatives, such as Type
639 M and Type S error, also rely upon calculation of p-values and definition of an arbitrary
640 alpha value, and are both a simple function of power (Gelman & Carlin, 2014). Type S
641 error (proportion of significant estimates that have the opposite sign) is not relevant for
642 variance components. Type M (absolute relative bias of significant estimates) gives some
643 additional information but, unlike power, it is affected by the measure of central tendency
644 that is chosen (Figure S11). Power can also be seen as a description of the distribution
645 of p-values expected for a given effect size and data structure. Other descriptions of this

646 distribution (e.g. the mean) would be simple functions of the power, but the common
647 use of this metric makes it more widely understood. An alternative to power would be to
648 design studies around a desired level of precision in estimates. Although this works for
649 unbounded parameters, precision is difficult to interpret for variance components, and
650 SE will decrease as true value gets closer to zero, not because precision increases, but
651 because it is limited by zero (see Figure S4). We would therefore suggest that power still
652 provides a suitable metric for designing studies to estimate variance components.

653 We show two methods of power analysis based upon null distributions. The first (full)
654 involves generating p-values for each simulated dataset by generating a null distribution
655 for that dataset. This method is highly computationally intensive as it involves running
656 a certain number of simulations multiplied by the number of permutations/simulations
657 models, which could realistically be one million models per parameter. Our alternative
658 method (reduced) is to generate a single null distribution for each data structure, and
659 generate p-values by comparing the parameter estimates from the simulated datasets to
660 this single null distribution. This method gives similar results to the first approach and
661 is massively less computationally intensive (requiring running 2000 models rather than
662 a million for each set of parameters). The disadvantage is that the false positive rate
663 cannot be calculated.

664 Even if power is not the intended use (or there is an objection to arbitrary alpha
665 values), these simulations can serve an extremely useful purpose before studies are con-
666 ducted. First, these simulations allow an empiricist to consider the distribution of p-values
667 expected under a given effect size and design (note power is essentially a description of
668 the shape of this distribution). Second, the null distribution of point estimates can be
669 considered - this enables the distribution of effect sizes that can occur under the null
670 hypothesis to be visualised. Even if an empiricist does not want to calculate a p-value,
671 creating a null distribution is still a powerful way of seeing the distribution of estimates
672 that would be generated with no among-group variance, and would serve to encourage

673 caution in how results that lie within that distribution are interpreted.

674 **6.5 Recommendations**

- 675 1. Use of posterior median as a measure of central tendency for posterior distributions
676 of variance components from MCMC-based models. Our results show that the
677 median is the least biased estimate, but will overestimate variances when power is
678 low. Reporting multiple measures of central tendency allows any asymmetry in the
679 posterior to be made obvious.
- 680 2. Reporting of smoothing values in kernel estimation. Kernel density estimation is
681 commonly used for estimating the posterior mode and creating density plots. The
682 parameters used in this estimation are seldom reported, but can have a large impact
683 on interpretation. We advise the reporting of parameters in the kernel density
684 estimation, or the use of more explicit methods of plotting posterior distributions,
685 such as histograms.
- 686 3. Using null distributions for inference. Null distributions provide a way of putting the
687 observed parameter estimates into a context expected under an explicitly defined
688 null hypothesis (i.e. no among-group variance). Null distributions can be created in
689 multiple ways, but they are most easily controlled when generated using simulations.
690 As with many aspects of statistical analysis, there are many decisions relating to
691 generating null distributions that may have an affect on the results. Therefore,
692 these methods should be defined pre-analysis, in order to reduce researcher degrees
693 of freedom.
- 694 4. Using a null distribution to estimating power. As well as aiding *post-hoc* inference,
695 null distributions can be used for power analysis. We provide details of a method
696 for doing so that does not present a large computational burden.

697 Acknowledgments

698 We would like to thank the other members of the Statistical Quantification of Individual
699 Differences (SQuID) working group, and the Wild Evolution and Statistics in Ecology
700 and Evolution Discussion groups at the University of Edinburgh for valuable feedback on
701 the ideas presented here. SQuID workshops in 2022 and JLP were funded by a Research
702 Council of Norway INTPART project number 309356 grant to JW. YGA was supported
703 by the Research Council of Norway project number 325826. HS were supported by
704 the German Research Foundation (DFG, 215/543-1, 316099922). DFW was supported
705 by the U.S. National Science Foundation. HA was supported by the Natural Sciences
706 and Engineering Research Council of Canada (CGSD3-504399-2017) and the Fond de
707 Recherche du Québec - Nature et Technologies (FRQNT; 283511).

708 References

- 709 Allegue, H., Araya-Ajoy, Y.G., Dingemanse, N.J., Dochtermann, N.A., Garamszegi, L.Z.,
710 Nakagawa, S., Réale, D., Schielzeth, H. & Westneat, D.F. (2017) Statistical Quantifi-
711 cation of Individual Differences (SQuID): an educational and statistical tool for under-
712 standing multilevel phenotypic data in linear mixed models. *Methods in Ecology and*
713 *Evolution*, **8**, 257–267. eprint: [https://onlinelibrary.wiley.com/doi/pdf/10.1111/2041-](https://onlinelibrary.wiley.com/doi/pdf/10.1111/2041-210X.12659)
714 [210X.12659](https://dx.doi.org/10.1111/2041-210X.12659), <https://dx.doi.org/10.1111/2041-210X.12659>.
- 715 Amrhein, V., Greenland, S. & McShane, B. (2019) Scientists rise up against statistical
716 significance. *Nature*, **567**, 305–307. <https://dx.doi.org/10.1038/d41586-019-00857-9>.
- 717 Amrhein, V., Korner-Nievergelt, F. & Roth, T. (2017) The earth is flat ($p > 0.05$):
718 Significance thresholds and the crisis of unreplicable research. *PeerJ*, **5**, e3544.
719 <https://dx.doi.org/10.7717/peerj.3544>.
- 720 Araya-Ajoy, Y.G. & Dingemanse, N.J. (2014) Characterizing behavioural 'characters':

721 an evolutionary framework. *Proceedings of the Royal Society of London Series B*, **281**,
722 20132645. <https://dx.doi.org/10.1098/rspb.2013.2645>.

723 Araya-Ajoy, Y.G. & Dingemanse, N.J. (2017) Repeatability, heritability, and age-
724 dependence of seasonal plasticity in aggressiveness in a wild passerine bird. *Journal of*
725 *Animal Ecology*, **86**, 227–238. <https://dx.doi.org/10.1111/1365-2656.12621>.

726 Bates, D., Mächler, M., Bolker, B. & Walker, S. (2015) Fitting linear
727 mixed-effects models using lme4. *Journal of Statistical Software*, **67**, 1–48.
728 <https://dx.doi.org/10.18637/jss.v067.i01>.

729 Bell, A.M., Hankison, S.J. & Laskowski, K.L. (2009) The repeatability of behaviour: a
730 meta-analysis. *Animal Behaviour*, **77**, 771–783. Publisher: Elsevier Ltd ISBN: 0003-
731 3472, <https://dx.doi.org/10.1016/j.anbehav.2008.12.022>.

732 Bolker, B.M., Brooks, M.E., Clark, C.J., Geange, S.W., Poulsen, J.R., Stevens,
733 M.H.H. & White, J.S.S. (2009) Generalized linear mixed models: A practical
734 guide for ecology and evolution. *Trends in Ecology and Evolution*, **24**, 127–135.
735 <https://dx.doi.org/10.1016/j.tree.2008.10.008>.

736 Bonnet, T., Morrissey, M.B., de Villemereuil, P., Alberts, S.C., Arcese, P., Bailey, L.D.,
737 Boutin, S., Brekke, P., Brent, L.J.N., Camenisch, G., Charmantier, A., Clutton-Brock,
738 T.H., Cockburn, A., Coltman, D.W., Courtiol, A., Davidian, E., Evans, S.R., Ewen,
739 J.G., Festa-Bianchet, M., de Franceschi, C., Gustafsson, L., Höner, O.P., Houslay,
740 T.M., Keller, L.F., Manser, M., McAdam, A.G., McLean, E., Nietlisbach, P., Osmond,
741 H.L., Pemberton, J.M., Postma, E., Reid, J.M., Rutschmann, A., Santure, A.W.,
742 Sheldon, B.C., Slate, J., Teplitsky, C., Visser, M.E., Wachter, B. & Kruuk, L.E.B.
743 (2022) Genetic variance in fitness indicates rapid contemporary adaptive evolution in
744 wild animals. *Science*, **376**, 1012–1016. <https://dx.doi.org/10.1126/science.abk0853>.

745 Cleasby, I.R., Nakagawa, S. & Schielzeth, H. (2015) Quantifying the predictability
746 of behaviour: Statistical approaches for the study of between-individual variation

- 747 in the within-individual variance. *Methods in Ecology and Evolution*, **6**, 27–37.
748 <https://dx.doi.org/10.1111/2041-210X.12281>.
- 749 de Villemereuil, P., Gimenez, O. & Doligez, B. (2013) Comparing parent–offspring re-
750 gression with frequentist and Bayesian animal models to estimate heritability in wild
751 populations: A simulation study for Gaussian and binary traits. *Methods in Ecology*
752 *and Evolution*, **4**, 260–275. <https://dx.doi.org/10.1111/2041-210X.12011>.
- 753 Dingemanse, N.J. & Dochtermann, N.A. (2013) Quantifying individual variation in be-
754 haviour: Mixed-effect modelling approaches. *Journal of Animal Ecology*, **82**, 39–54.
755 <https://dx.doi.org/10.1111/1365-2656.12013>.
- 756 Fay, R., Authier, M., Hamel, S., Jenouvrier, S., van de Pol, M., Cam, E., Gaillard, J.M.,
757 Yoccoz, N.G., Acker, P., Allen, A., Aubry, L.M., Bonenfant, C., Caswell, H., Coste,
758 C.F.D., Larue, B., Le Coeur, C., Gamelon, M., Macdonald, K.R., Moiron, M., Nicol-
759 Harper, A., Pelletier, F., Rotella, J.J., Teplitsky, C., Touzot, L., Wells, C.P. & Sæther,
760 B.E. (2022) Quantifying fixed individual heterogeneity in demographic parameters:
761 Performance of correlated random effects for Bernoulli variables. *Methods in Ecology*
762 *and Evolution*, **13**, 91–104. <https://dx.doi.org/10.1111/2041-210X.13728>.
- 763 Fitzmaurice, G.M., Lipsitz, S.R. & Ibrahim, J.G. (2007) A Note on Permutation Tests
764 for Variance Components in Multilevel Generalized Linear Mixed Models. *Biometrics*,
765 **63**, 942–946. <https://dx.doi.org/10.1111/j.1541-0420.2007.00775.x>.
- 766 Gelman, A., Carlin, J.B., Stern, H.S., Dunson, D.B., Vehtari, A. & Rubin, D.B. (2013)
767 *Bayesian Data Analysis*. Chapman and Hall/CRC, 3rd edition.
- 768 Gelman, A., Hill, J. & Vehtari, A. (2020) *Regression and Other Stories*. Cambridge
769 University Press, Cambridge.
- 770 Gelman, A. (2006) Prior distributions for variance parameters in hierarchical models.
771 *Bayesian Analysis*, **1**, 515–533.

- 772 Gelman, A. & Carlin, J. (2014) Beyond Power Calculations: Assessing Type S (Sign)
773 and Type M (Magnitude) Errors. *Perspectives on Psychological Science*, **9**, 641–651.
774 <https://dx.doi.org/10.1177/1745691614551642>.
- 775 Gilks, W.R., Thomas, A. & Spiegelhalter, D.J. (1994) A Language and Program for
776 Complex Bayesian Modelling. *Journal of the Royal Statistical Society Series D (The*
777 *Statistician)*, **43**, 169–177. <https://dx.doi.org/10.2307/2348941>.
- 778 Hadfield, J.D. (2010) MCMC methods for multi-response generalized linear mixed mod-
779 els: The {MCMCglmm} {R} package. *Journal of Statistical Software*, **33**, 1–22.
780 <https://dx.doi.org/10.1002/ana.23792>.
- 781 Hadfield, J.D. & Nakagawa, S. (2010) General quantitative genetic methods for
782 comparative biology: Phylogenies, taxonomies and multi-trait models for contin-
783 uous and categorical characters. *Journal of Evolutionary Biology*, **23**, 494–508.
784 <https://dx.doi.org/10.1111/j.1420-9101.2009.01915.x>.
- 785 Harrison, X.A., Donaldson, L., Correa-Cano, M.E., Evans, J., Fisher, D.N., Good-
786 win, C.E.D., Robinson, B.S., Hodgson, D.J. & Inger, R. (2018) A brief introduction
787 to mixed effects modelling and multi-model inference in ecology. *PeerJ*, **6**, e4794.
788 <https://dx.doi.org/10.7717/peerj.4794>.
- 789 Held, L. & Sabanés Bové, D. (2020) *Likelihood and Bayesian Inference*, volume 10.
790 Springer.
- 791 Henderson, C.R. (1988) Theoretical basis and computational methods for a number of d-
792 ifferent animal models. *Journal of Dairy Science*, **71**, 1–16.
- 793 Houle, D. (1992) Comparing evolvability and variability of quantitative traits. *Genetics*,
794 **130**, 195–204. <https://dx.doi.org/citeulike-article-id:10041224>.
- 795 Kay, M. (2022) *ggdist: Visualizations of Distributions and Uncertainty*. R package version
796 3.2.0.

- 797 Kruschke, J. (2015) *Doing Bayesian Data Analysis*. Academic Press/Elsevier, second
798 edition.
- 799 Kruschke, J. (2018) Rejecting or Accepting Parameter Values in Bayesian Estima-
800 tion. *Advances in Methods and Practices in Psychological Science*, **1**, 270–280.
801 <https://dx.doi.org/10.1177/2515245918771304>.
- 802 Kruuk, L.E.B. (2004) Estimating genetic parameters in natural populations using the
803 “animal model”. *Philosophical Transactions of the Royal Society of London B*, **359**,
804 873–890. <https://dx.doi.org/10.1098/rstb.2003.1437>.
- 805 Lakens, D., Scheel, A.M. & Isager, P.M. (2018) Equivalence Testing for Psychological
806 Research: A Tutorial. *Advances in Methods and Practices in Psychological Science*, **1**,
807 259–269. <https://dx.doi.org/10.1177/2515245918770963>.
- 808 Lehmann, E.L. & Romano, J.P. (2005) *Testing Statistical Hypotheses*. Springer Texts in
809 Statistics. Springer, New York, 3rd ed edition.
- 810 Lemoine, N.P. (2019) Moving beyond noninformative priors: Why and how to
811 choose weakly informative priors in Bayesian analyses. *Oikos*, **128**, 912–928.
812 <https://dx.doi.org/10.1111/oik.05985>.
- 813 Makowski, D., Ben-Shachar, M.S., Chen, S.H.A. & Lüdtke, D. (2019a) Indices of Effect
814 Existence and Significance in the Bayesian Framework. *Frontiers in Psychology*, **10**,
815 2767. <https://dx.doi.org/10.3389/fpsyg.2019.02767>.
- 816 Makowski, D., Ben-Shachar, M.S. & Lüdtke, D. (2019b) bayestestr: Describing effects
817 and their uncertainty, existence and significance within the bayesian framework. *Jour-
818 nal of Open Source Software*, **4**, 1541. <https://dx.doi.org/10.21105/joss.01541>.
- 819 McElreath, R. (2020) *Statistical Rethinking: A Bayesian Course with Examples in R and
820 Stan*. Chapman and Hall/CRC, 2nd edition.

- 821 McFarlane, S.E., Gorrell, J.C., Coltman, D.W., Humphries, M.M., Boutin, S. & Mcadam,
822 A.G. (2015) The nature of nurture in a wild mammal's fitness. *Proceedings of the Royal*
823 *Society of London B*, **282**, 1–7.
- 824 McShane, B.B., Gal, D., Gelman, A., Robert, C. & Tackett, J.L. (2019)
825 Abandon Statistical Significance. *The American Statistician*, **73**, 235–245.
826 <https://dx.doi.org/10.1080/00031305.2018.1527253>.
- 827 Morey, R.D., Romeijn, J.W. & Rouder, J.N. (2016) The philosophy of bayes factors and
828 the quantification of statistical evidence. *Journal of Mathematical Psychology*, **72**,
829 6–18. <https://dx.doi.org/10.1016/j.jmp.2015.11.001>.
- 830 Nakagawa, S. & Schielzeth, H. (2010) Repeatability for Gaussian and non-Gaussian data:
831 A practical guide for biologists. *Biological Reviews of the Cambridge Philosophical*
832 *Society*, **85**, 935–56. <https://dx.doi.org/10.1111/j.1469-185X.2010.00141.x>.
- 833 Navarro, D.J. (2019) Between the Devil and the Deep Blue Sea: Tensions Between Sci-
834 entific Judgement and Statistical Model Selection. *Computational Brain & Behavior*,
835 **2**, 28–34. <https://dx.doi.org/10.1007/s42113-018-0019-z>.
- 836 O'Hara, R.B., Cano, J.M., Ovaskainen, O., Teplitsky, C. & Alho, J.S. (2008) Bayesian
837 approaches in evolutionary quantitative genetics. *Journal of Evolutionary Biology*, **21**,
838 949–957. <https://dx.doi.org/10.1111/j.1420-9101.2008.01529.x>.
- 839 O'Hara, R.B. & Merilä, J. (2005) Bias and precision in QST esti-
840 mates: Problems and some solutions. *Genetics*, **171**, 1331–1339.
841 <https://dx.doi.org/10.1534/genetics.105.044545>.
- 842 Pesarin, F. & Salmaso, L. (2010) *Permutation Tests for Complex Data*. John Wiley &
843 Sons, Ltd, first edition.
- 844 Pick, J.L. (2022) *squidSim: a flexible simulation tool for linear mixed models*. R package
845 version 0.1.0.

846 Plummer, M. (2003) Jags: A program for analysis of bayesian graphical models using
847 gibbs sampling. *3rd International Workshop on Distributed Statistical Computing (DSC*
848 *2003); Vienna, Austria*, **124**.

849 R Core Team (2022) *R: A Language and Environment for Statistical Computing*. R
850 Foundation for Statistical Computing, Vienna, Austria.

851 Ramakers, J.J.C., Visser, M.E. & Gienapp, P. (2020) Quantifying individual variation
852 in reaction norms: Mind the residual. *Journal of Evolutionary Biology*, **33**, 352–366.
853 <https://dx.doi.org/10.1111/jeb.13571>.

854 Samuh, M.H., Grilli, L., Rampichini, C., Salmaso, L. & Lunardon, N. (2012)
855 The Use of Permutation Tests for Variance Components in Linear Mixed Mod-
856 els. *Communications in Statistics - Theory and Methods*, **41**, 3020–3029.
857 <https://dx.doi.org/10.1080/03610926.2011.587933>.

858 Schad, D.J., Nicenboim, B., Bürkner, P.C., Betancourt, M. & Vasishth, S. (2022) Work-
859 flow techniques for the robust use of bayes factors. *Psychological Methods*, pp. No
860 Pagination Specified–No Pagination Specified. Place: US Publisher: American Psy-
861 chological Association, <https://dx.doi.org/10.1037/met0000472>.

862 Schwaferts, P. & Augustin, T. (2020) Bayesian decisions using regions of practical equiv-
863 alence (rope): Foundations.

864 Sheather, S.J. & Jones, M.C. (1991) A Reliable Data-Based Bandwidth Selection Method
865 for Kernel Density Estimation. *Journal of the Royal Statistical Society Series B*
866 *(Methodological)*, **53**, 683–690.

867 Silverman, B.W. (1986) *Density Estimation for Statistics and Data Analysis*. Chapman
868 and Hall, London.

869 Stan Development Team (2022a) RStan: the R interface to Stan. R package version
870 2.21.3.

- 871 Stan Development Team (2022b) Stan modeling language users guide and reference man-
872 ual. Version 2.3.
- 873 Stoffel, M.A., Nakagawa, S. & Schielzeth, H. (2017) rptR: Repeatability estimation and
874 variance decomposition by generalized linear mixed-effects models. *Methods in Ecology*
875 *and Evolution*, **8**, 1639–1644. <https://dx.doi.org/10.1111/2041-210X.12797>.
- 876 Wasserstein, R.L. & Lazar, N.A. (2016) The ASA Statement on p-Values:
877 Context, Process, and Purpose. *The American Statistician*, **70**, 129–133.
878 <https://dx.doi.org/10.1080/00031305.2016.1154108>.

7 Figures

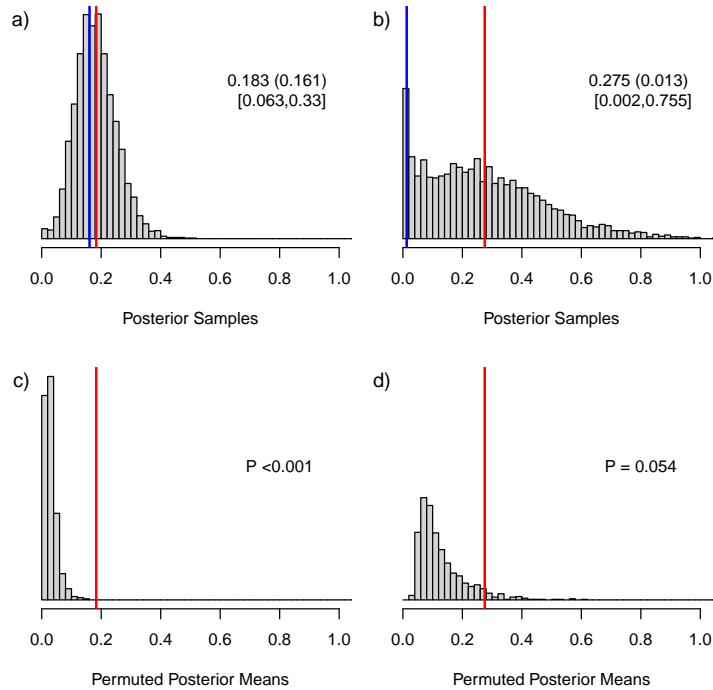


Figure 1: Posterior distributions of variance estimates for two different scenarios (a and b) and their respective null distributions (c and d) generated using permutations. Example a) shows a symmetric posterior distribution far away from zero with close agreement between the posterior mean (red lines) and mode (blue line), whilst b) shows an asymmetric posterior distribution close to zero, with clear divergence between the posterior mean and mode. c) and d) show null distributions of posterior means generated through permuting the datasets, and corresponding p-values, of a) and b), respectively. The values given in a) and b) correspond to mean (mode) [CRIs]. Both datasets were simulated with among-group variances of 0.2, but with differing sample sizes; a) with 80 groups and 4 observations per group; b) with 40 groups and 2 observations per group.

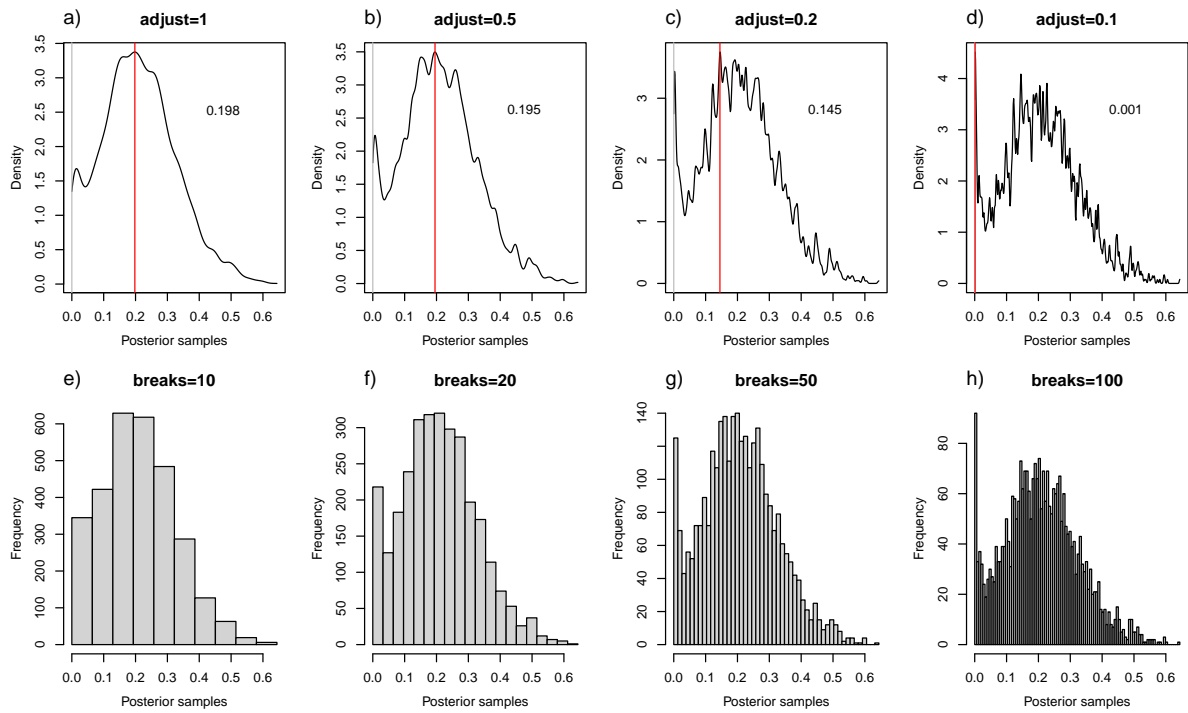


Figure 2: The effect of bandwidth choice on the estimation of the posterior mode. Top row shows kernel densities of the same posterior distribution, estimated with different bandwidth scalings, from 1 in a) to 0.1 in d). Red lines shows the posterior modes estimated from that scaling. Bottom row shows the equivalent histograms for comparison.

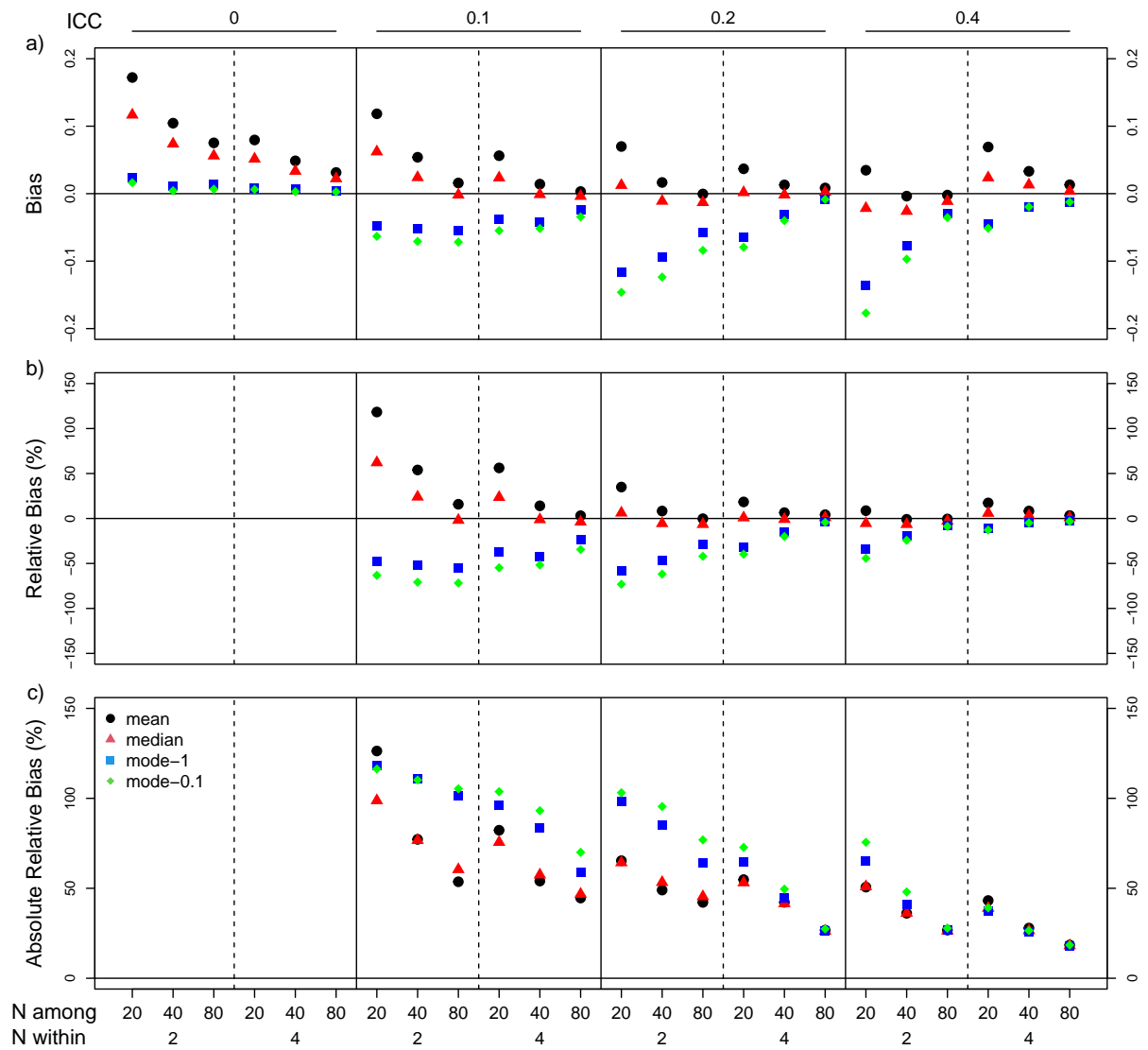


Figure 3: Bias (a), relative bias (b) and absolute relative bias (c) of posterior mean, median and mode of variance components from simulations varying in among group variance (ICC - 0, 0.1, 0.2, and 0.4) and sample size within (2 or 4) and among (20, 40, 80) groups. Two posterior modes were estimated: mode-1 and mode-0.1 with more and less smoothing, respectively (see text for more details).

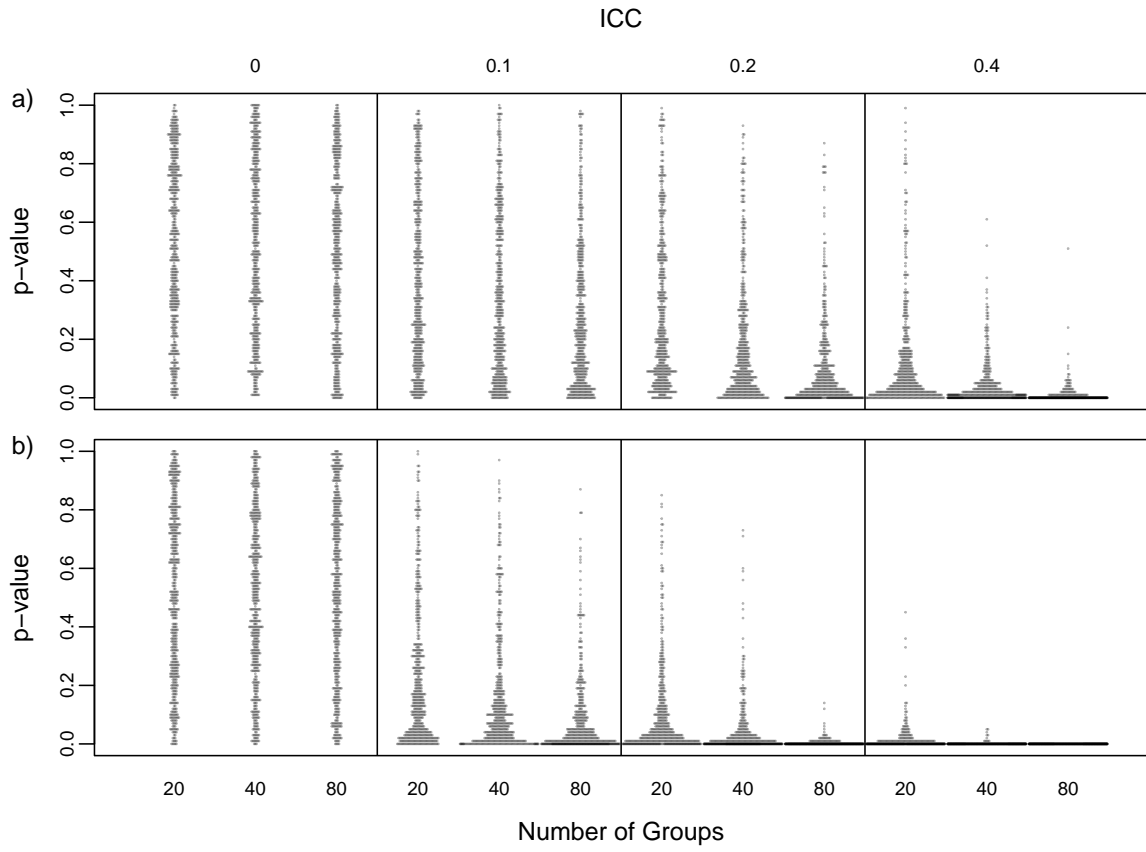


Figure 4: Distribution of p -values estimated using the posterior median and null distributions generated through simulations for datasets varying in among-group variance ($ICC = 0, 0.1, 0.2, \text{ and } 0.4$) and sample size among (20, 40, 80) groups. Example a) shows a within group sample size of 2, and b) a within group sample size of 4.

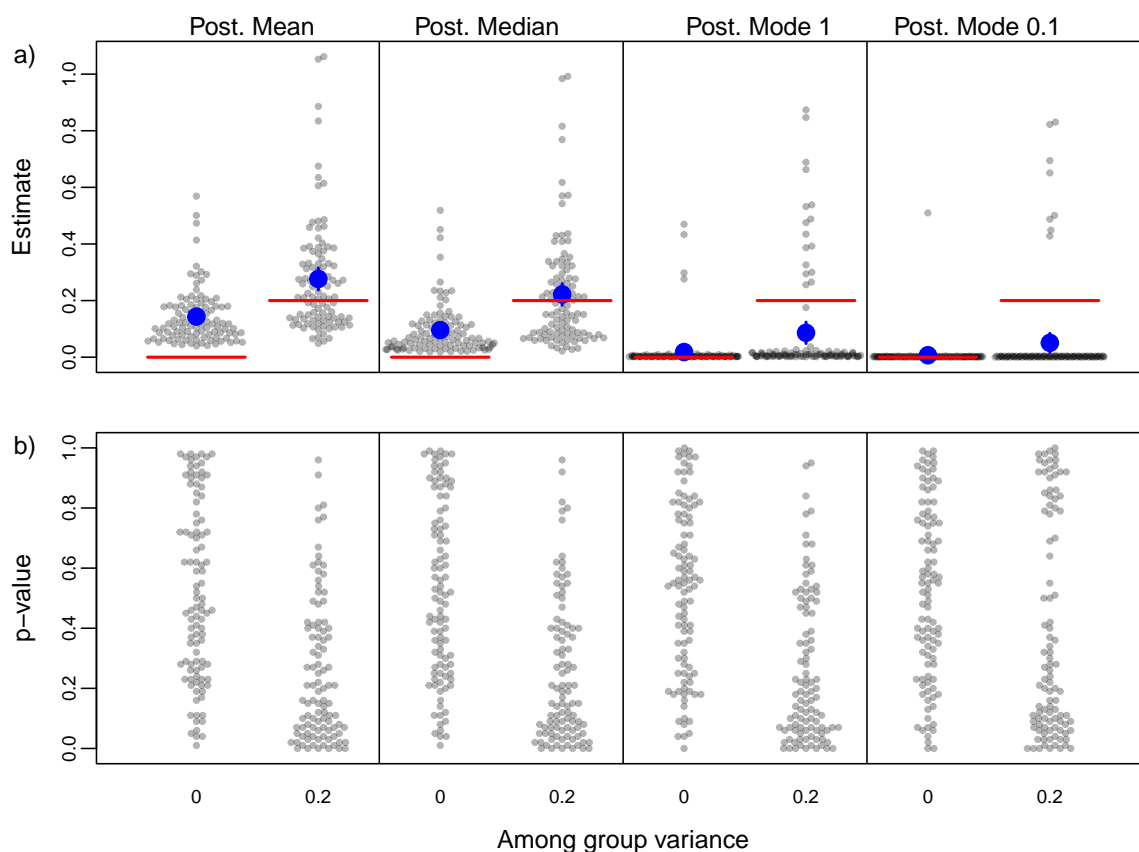


Figure 5: Sampling distributions of parameter estimates (a) and p-values (b) from GLMMs using different measures of central tendency. Two posterior modes were estimated: mode-1 and mode-0.1 with more and less smoothing, respectively (see text for more details). In a) red lines show simulated values, and blue points and error bars show mean and standard error of the sampling distributions. The p-values were generated using null distributions generated through simulation.

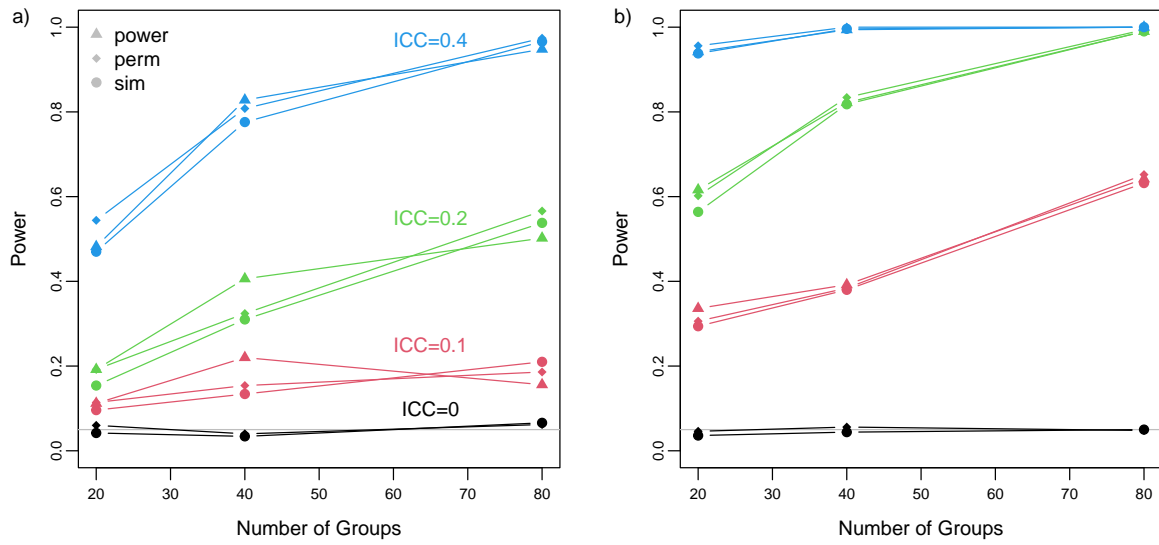


Figure 6: Comparisons of power calculated using permutation (*perm*), simulation (*sim*) or a global null distribution (*power*). For each within-group sample size of a) 2 and b) 4, we show results for four among-group variances (0, 0.1, 0.2 and 0.4) and three among-group sample sizes (20, 40 and 80). Power was calculated using posterior medians.

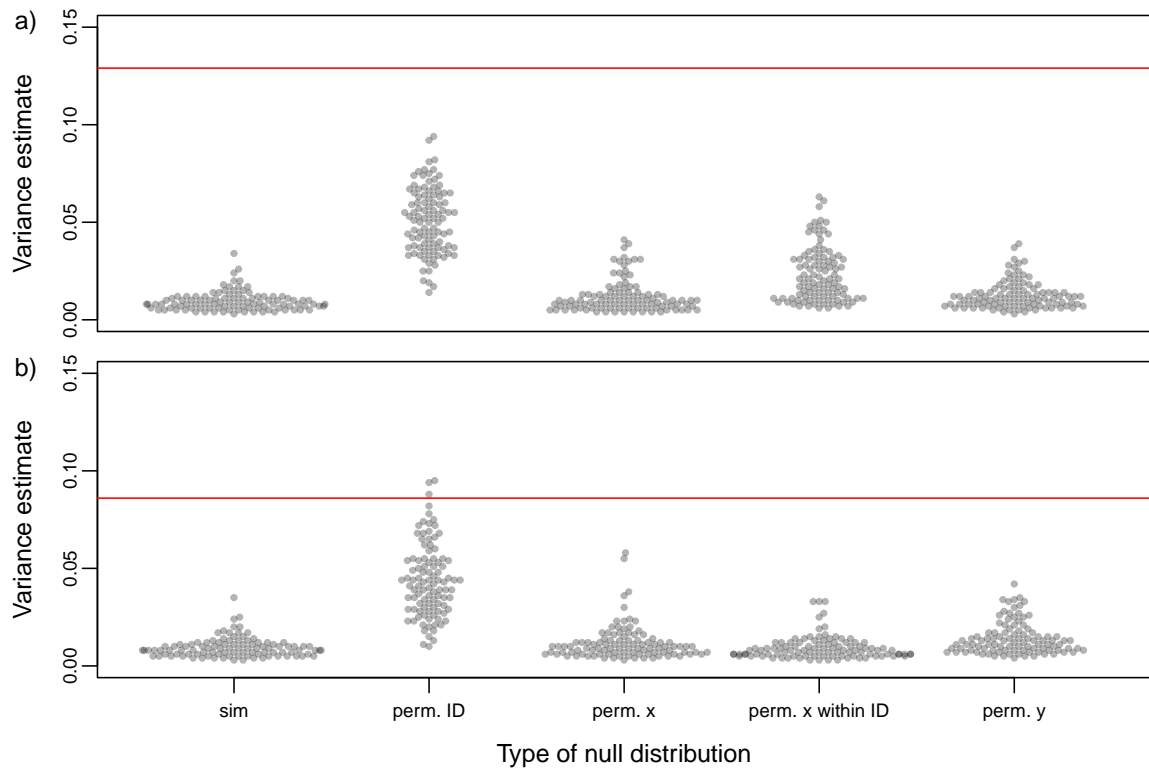


Figure 7: Null distributions of posterior medians generated with five different methods (see main text), from a) a simulated dataset, and b) a real dataset on aggressiveness in great tits. Red line represents posterior median estimated from original dataset.

880 **Supplementary Materials**

881 **Supplementary Methods**

882 **Simulations based on [Fay et al. \(2022\)](#)**

883 We simulated datasets based on [Fay et al. \(2022\)](#), but ran simplified models (univariate
884 instead of bivariate), as the purpose was simply to demonstrate the effect of different
885 measures of central tendency on the bias in these models. We simulated data with the
886 same parameters of one set of simulation in [Fay et al. \(2022\)](#) - fast life history and
887 low heterogeneity. We simulated the probability of survival as 0.5 and probability of
888 reproduction as 0.7, standard deviations on the latent scale of 0.2 for both survival and
889 reproduction and a correlation of 0.6 between the two. We simulated 100 datasets from
890 sample sizes of 250, 500, 1000, 2000, 4000 individuals. For each simulated dataset we ran
891 a binomial GLMM, with random effects of individual identity using Stan with the rstan
892 package (version 2.21.3 [Stan Development Team, 2022a](#)). We specified weakly informative
893 priors on the among-group standard deviations (half-Cauchy distribution with scale 2),
894 and ran one chain for each model with 7500 iterations and a warm-up period of 2000
895 iterations. We then estimated the posterior mean, median and 2 modes as in the main
896 text.

897 **Supplementary Figures**

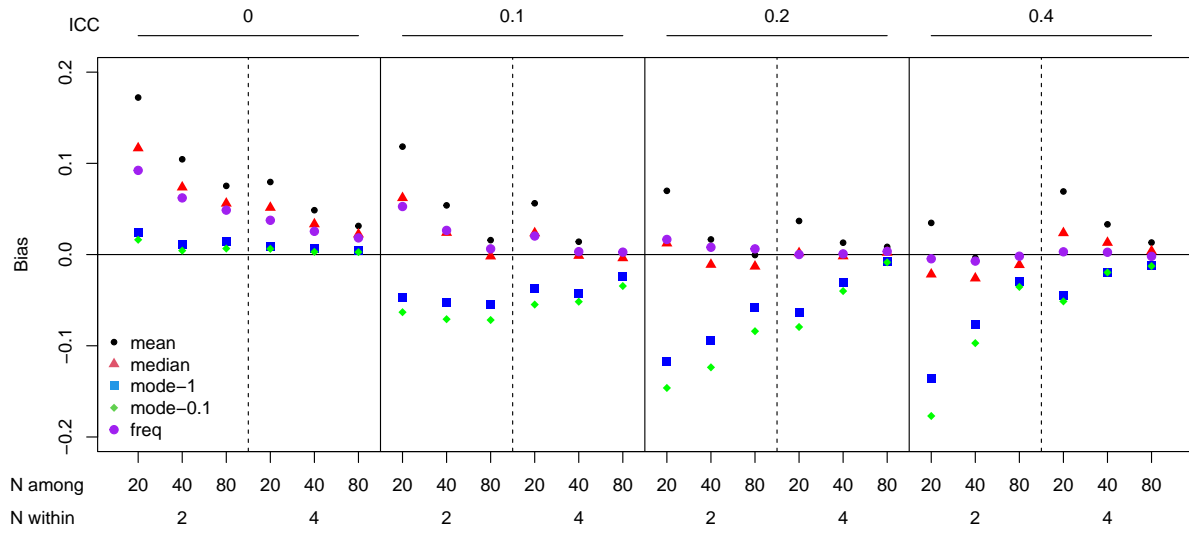


Figure S1: Bias of Frequentist estimates alongside posterior mean, median and mode of variance components, from simulations varying in among-group variance (ICC - 0, 0.1, 0.2, and 0.4) and sample size within (2 or 4) and among (20, 40, 80) groups. Two posterior modes were estimated; mode-1 and mode-0.1 with more and less smoothing, respectively (see text for more details).

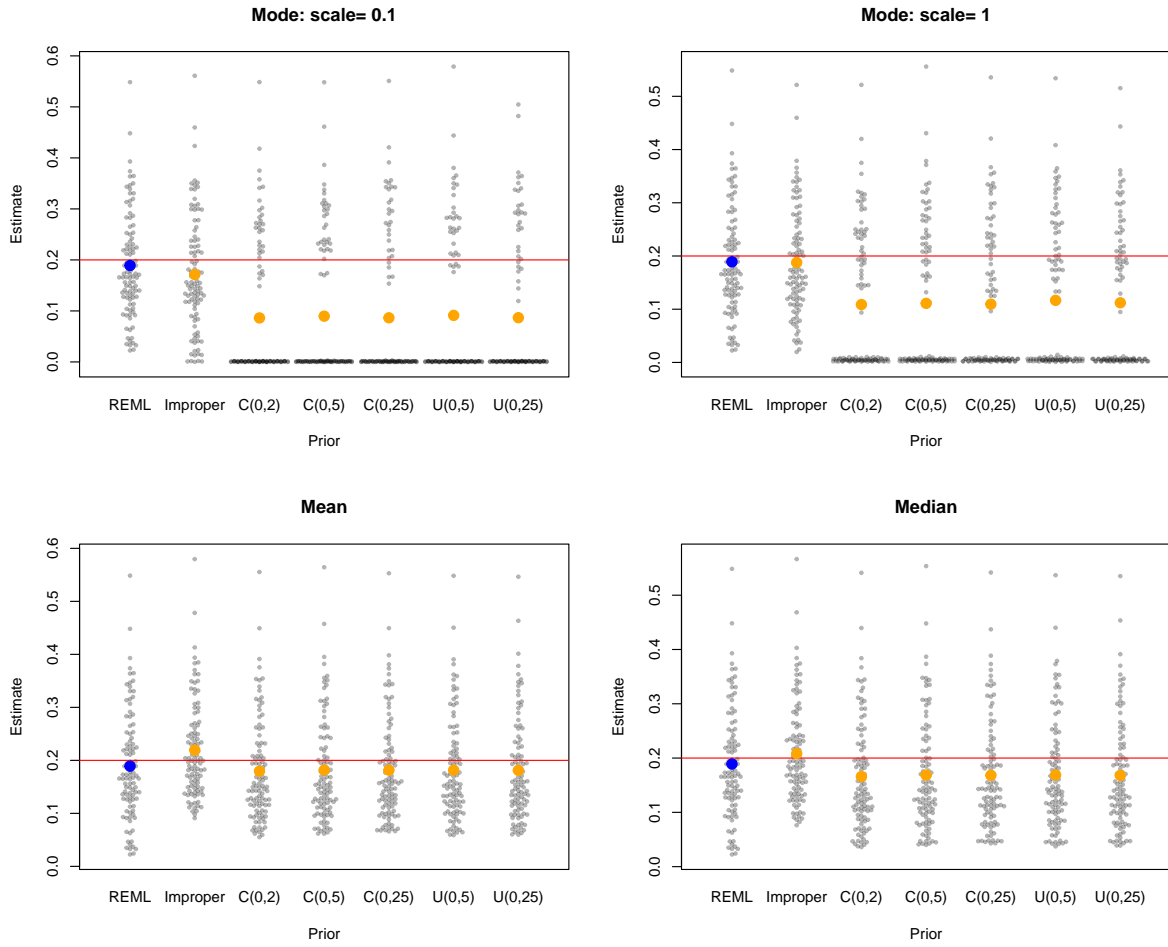


Figure S2: Impact of prior choice on measures of central tendency. 'C' represents half Cauchy priors, 'U' uniform priors, and 'Improper' uninformative improper prior. Red lines shows simulated values, and orange points shows means of different point estimates from across simulations, and blue points show the mean of the REML estimates across simulations.

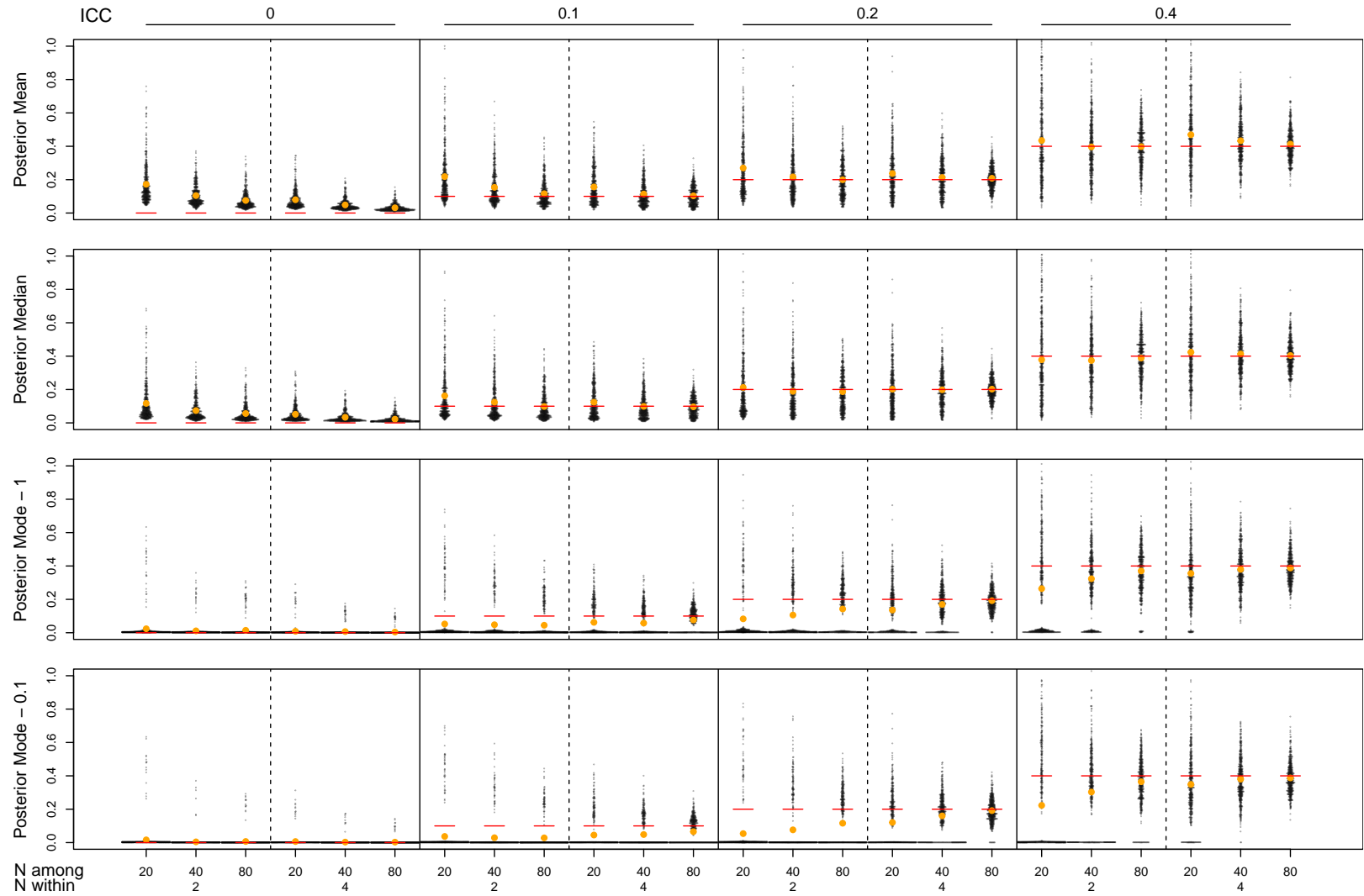


Figure S3: Sampling distributions of posterior mean, median and mode from simulations varying in among-group variance (ICC - 0, 0.1, 0.2, and 0.4) and sample size within (2 or 4) and among (20, 40, 80) groups. Red lines show the simulated value and orange points the mean of the sampling distributions.

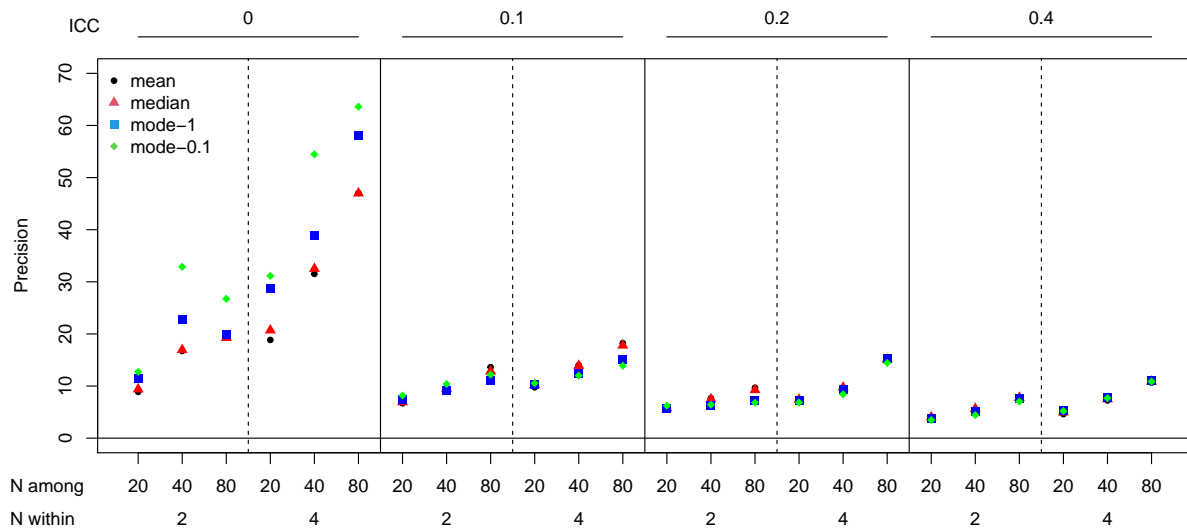


Figure S4: Precision increases with sample size, but decreases with effect size. The different panels show the precision of posterior mean, median and mode of variance components from simulations varying in among-group variance (ICC - 0, 0.1, 0.2, and 0.4) and sample size within (2 or 4) and among (20, 40, 80) groups. Two posterior modes were estimated; mode-1 and mode-0.1 with more and less smoothing, respectively (see text for more details).

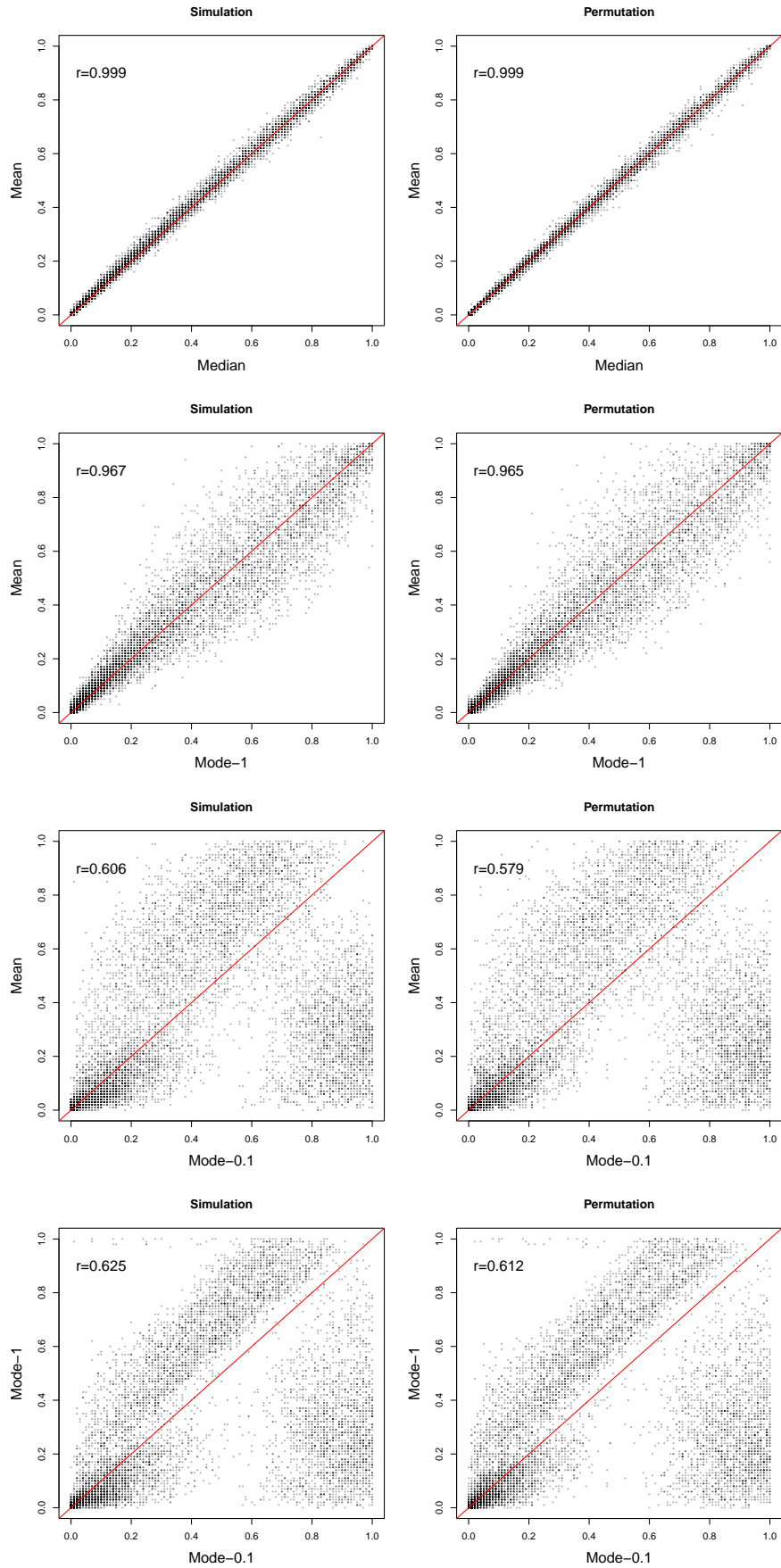


Figure S5: Comparison of p-values generated with different measures of central tendency using both simulations and permutations.

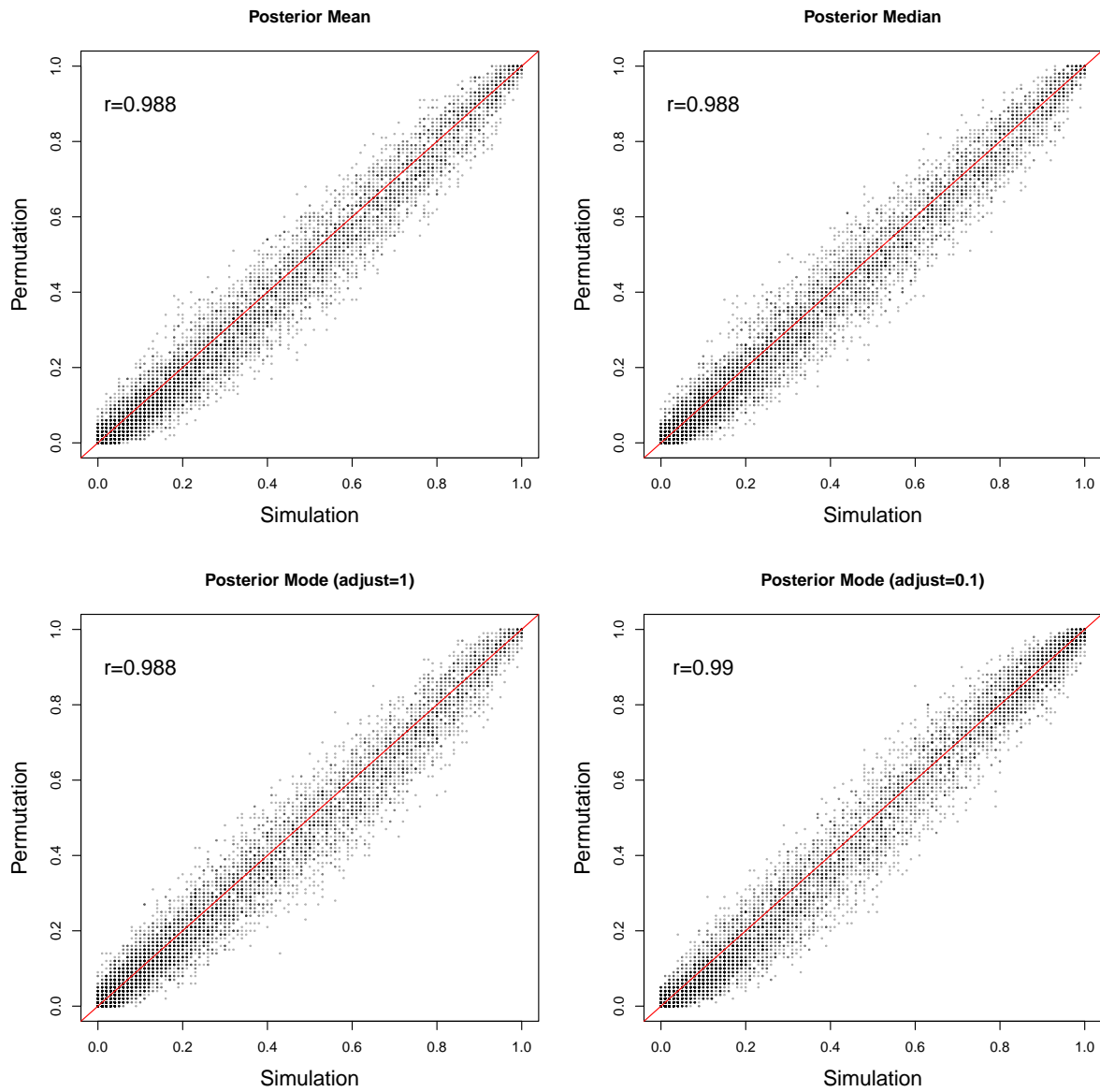


Figure S6: Comparison of p-values generated using permutation and simulation methods across all measures of central tendency.

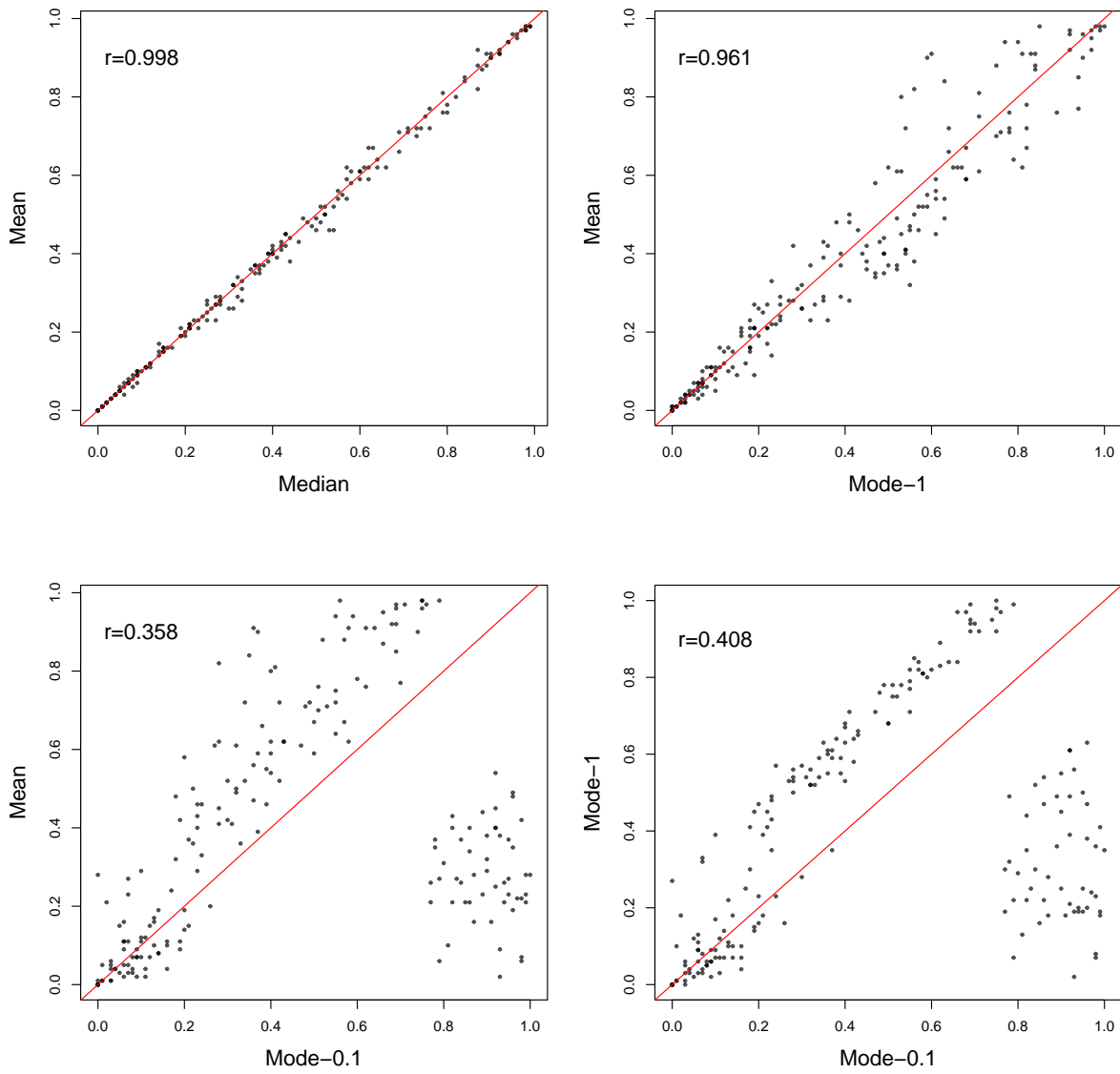


Figure S7: Comparison of p-values generated with different measures of central tendency from GLMMs using null distributions generated by simulation.

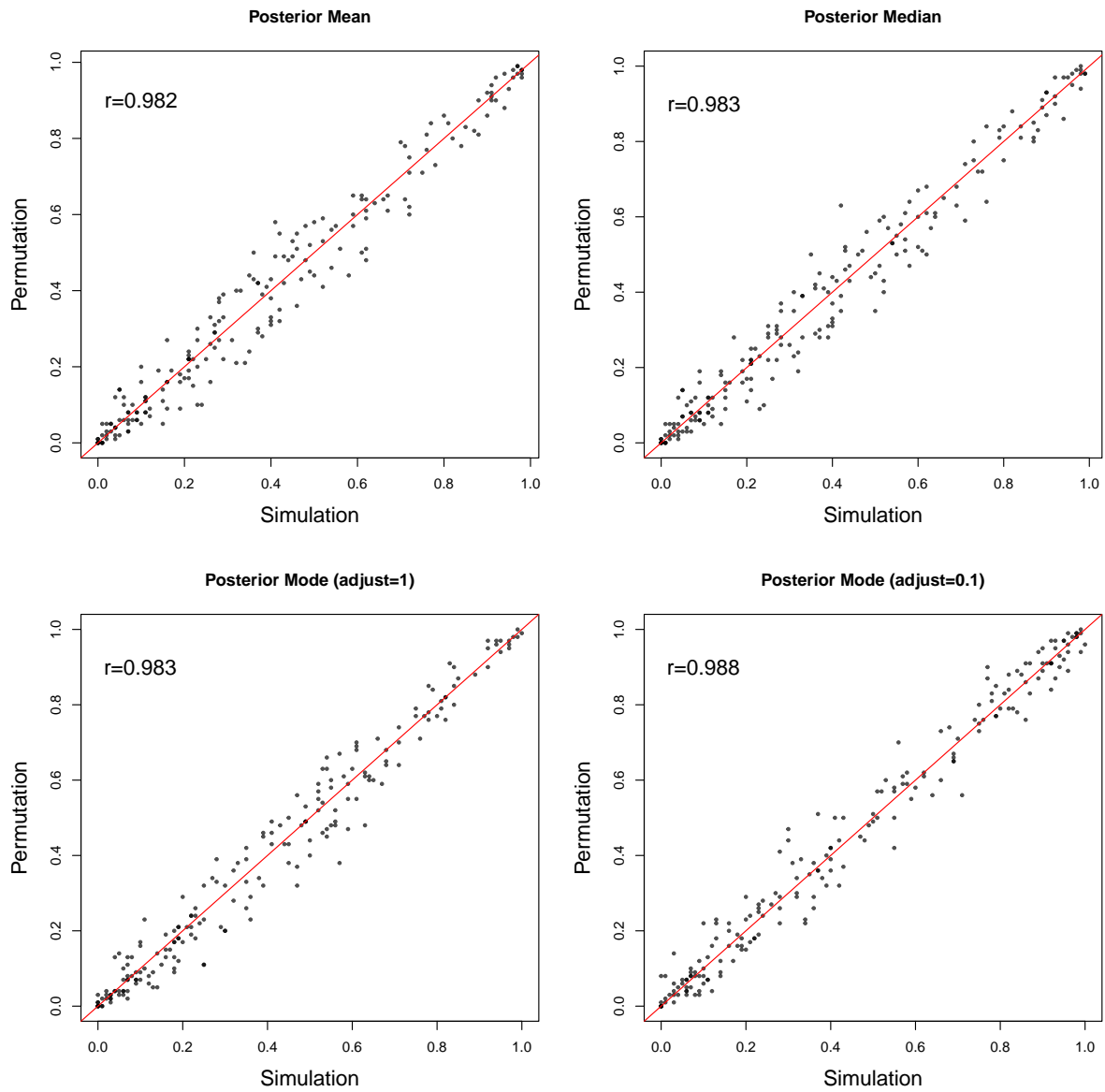


Figure S8: Comparison of p-values from GLMMs generated using permutation and simulation methods across all measures of central tendency.

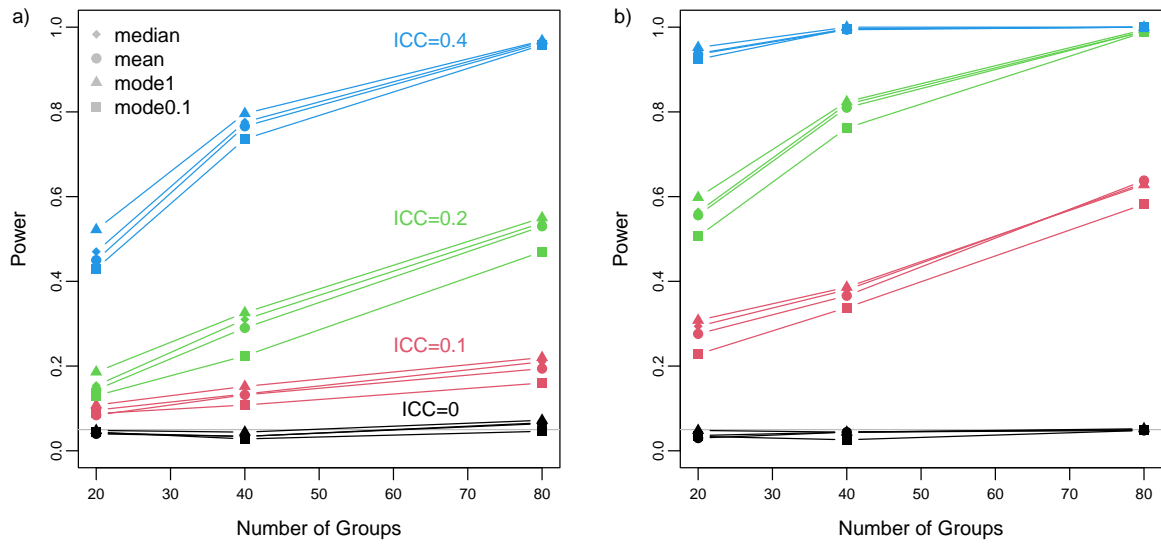


Figure S9: Comparison of power among different measures of central tendency

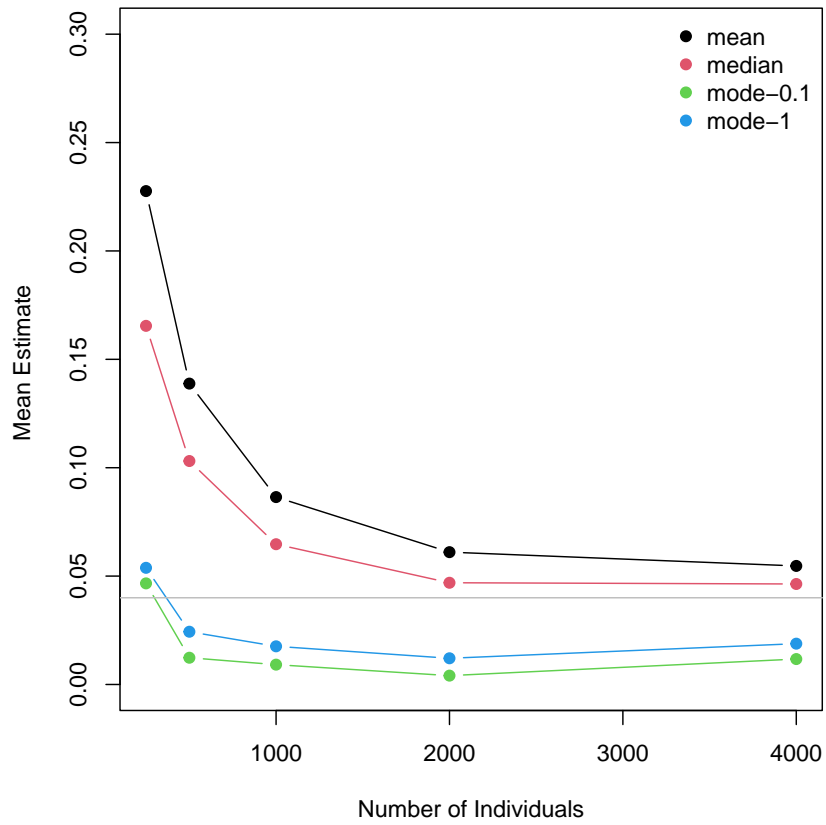


Figure S10: Mean posterior mean, median and mode of variance components from simulations based upon [Fay et al. \(2022\)](#).

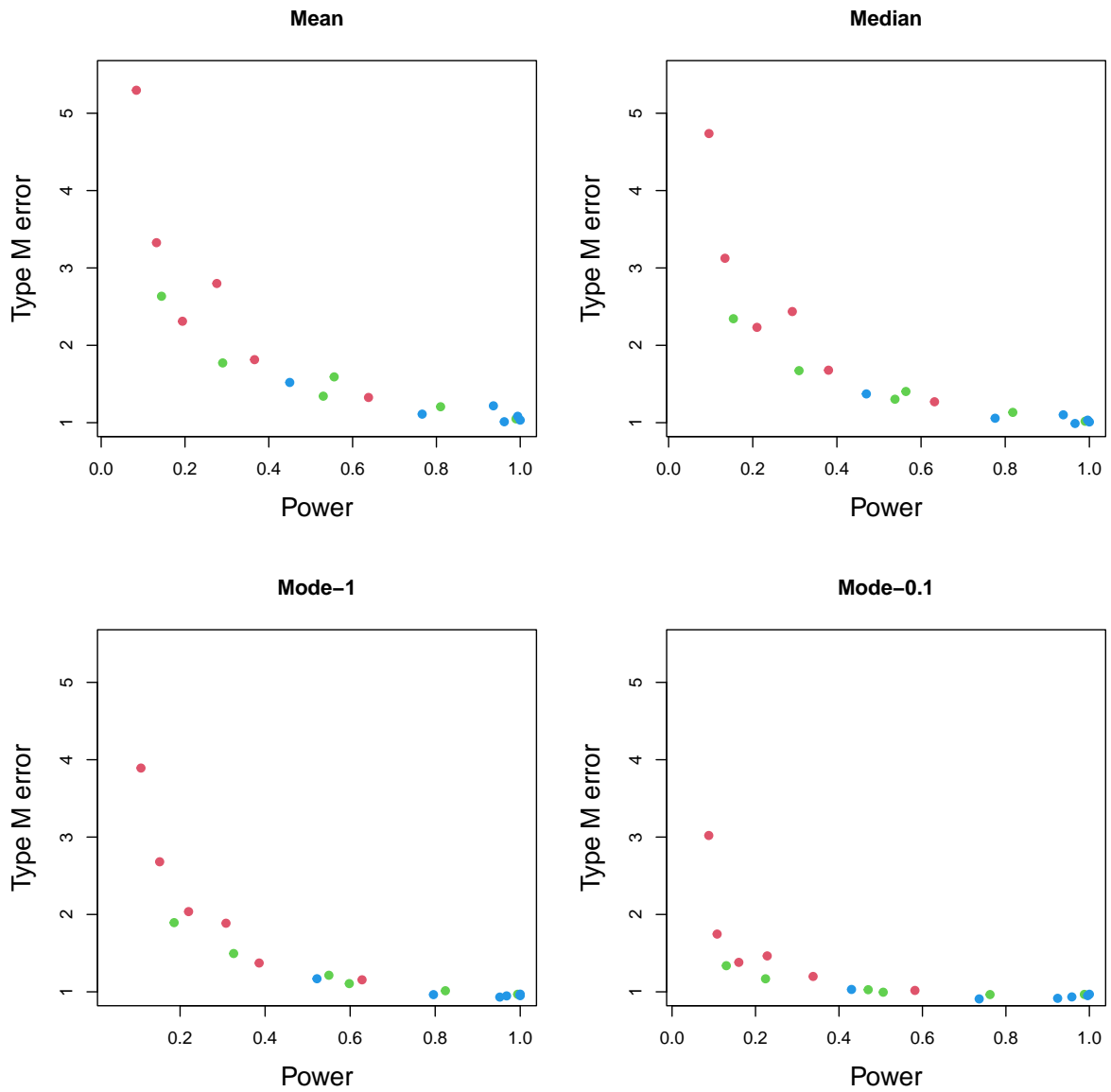


Figure S11: Type M error and power from posterior mean, median and mode calculated using null distribution generated through simulation. Colours represent simulated ICCs, red - 0.1, green - 0.2, and blue - 0.4.